Please cite this article in press as: Compan et al., Cell Volume Regulation Modulates NLRP3 Inflammasome Activation, Immunity (2012), http://dx.doi.org/10.1016/j.immuni.2012.06.013

Immunity
Article

Cell Volume Regulation Modulates NLRP3 Inflammasome Activation

Vincent Compan,[1] Alberto Baroja-Mazo,[2] Gloria López-Castejón,[1] Ana I. Gomez,[2] Carlos M. Martínez,[2] Diego Angosto,[3] María T. Montero,[4] Antonio S. Herranz,[4] Eulalia Bazán,[4] Diana Reimers,[4] Victoriano Mulero,[3] and Pablo Pelegrín[1,2,*]
[1]Faculty of Life Sciences, University of Manchester, Manchester M13 9PT, UK
[2]Inflammation and Experimental Surgery Unit, Centro de Investigación Biomédica en Red en el Área temática de Enfermedades Hepáticas y Digestivas (CIBERehd), Murcia Biomedical Research Institute (IMIB), University Hospital Virgen de la Arrixaca—Fundación para la Formación e Investigación Sanitarias de la Región de Murcia, 30120 Murcia, Spain
[3]Department of Cell Biology and Histology, Faculty of Biology, University of Murcia, 30100 Murcia, Spain
[4]Neurobiology Service, Hospital Ramón y Cajal, 28034 Madrid, Spain
*Correspondence: pablo.pelegrin@ffis.es
http://dx.doi.org/10.1016/j.immuni.2012.06.013

SUMMARY

Cell volume regulation is a primitive response to alterations in environmental osmolarity. The NLRP3 inflammasome is a multiprotein complex that senses pathogen- and danger-associated signals. Here, we report that, from fish to mammals, the basic mechanisms of cell swelling and regulatory volume decrease (RVD) are sensed via the NLRP3 inflammasome. We found that a decrease in extracellular osmolarity induced a K^+-dependent conformational change of the preassembled NLRP3-inactive inflammasome during cell swelling, followed by activation of the NLRP3 inflammasome and caspase-1, which was controlled by transient receptor potential channels during RVD. Both mechanisms were necessary for interleukin-1β processing. Increased extracellular osmolarity prevented caspase-1 activation by different known NLRP3 activators. Collectively, our data identify cell volume regulation as a basic conserved homeostatic mechanism associated with the formation of the NLRP3 inflammasome and reveal a mechanism for NLRP3 inflammasome activation.

INTRODUCTION

Changes in cell volume have been adapted to function as specific signals for the regulation of important physiological processes (Hoffmann et al., 2009; Lang et al., 1998). In many physiological conditions, cells exhibit rapid volume-regulatory mechanisms to recover their functionality in response to different signals, and alterations in osmosensing or osmosignaling are associated with a variety of pathophysiological conditions (Lang et al., 1998). Cell swelling has been reported to occur during different clinical situations such as hypoxia, ischemia, hyponatremia, hypothermia, and in intracellular acidosis and diabetic ketoacidosis (Hoffmann et al., 2009; Newman and Grana, 1988). Cell volume regulation is of prime importance to the CNS because of the restricted volume of the skull, and current clinical treatment of stroke aims to reduce intracranial pressure by administration of hypertonic solutions (Jain, 2008).

Interleukin-1β (IL-1β) influences the pathogenesis and course of brain diseases, such as epilepsy, or brain injuries, such as stroke (Li et al., 2011; Rothwell, 2003). IL-1β release is tightly regulated by the inflammasome, a multiprotein complex that activates caspase-1, the enzyme responsible for generating the mature bioactive form of IL-1β (Schroder and Tschopp, 2010). NLRP3 (nucleotide-binding domain and leucine-rich repeat pyrin 3 domain) oligomerizes and assembles with ASC (apoptosis-associated speck-like protein containing a caspase recruitment domain) to form functional inflammasomes in response to a wide range of extracellular danger signals, including ATP or crystals. The NLRP3 inflammasome is positively regulated by low intracellular K^+, by increased reactive oxygen species, and by lysosome membrane disruption (Hornung et al., 2008; Schroder and Tschopp, 2010; Zhou et al., 2010), all of which are processes affected during cell swelling (Hoffmann et al., 2009). Inflammasomes not only regulate immune cells, but are also functional in other cell types, such as neurons, keratinocytes, or pancreatic β cells, and generate an integrated host effector response (de Rivero Vaccari et al., 2008; Feldmeyer et al., 2007; Zhou et al., 2010).

An anisosmotic condition represents an important and conserved danger signal, which, in the case of hypotonicity, induces processing and release of IL-1β (Perregaux et al., 1996). Recently, it has been reported that activation of the NLRP3 inflammasomme by uric acid (monosodium urate, MSU) crystal is associated with water influx that leads to cell swelling (Schorn et al., 2011). We found that low osmolarities induced macrophage swelling and a decrease in intracellular K^+ and Cl^- concentrations, which activated a regulatory volume decrease (RVD) process controlled by a transient receptor potential (TRP) channel with a pharmacology profile close to TRP melastatin 7 (TRPM7). During RVD, TRP vanilloid 2 (TRPV2) was translocated to the plasma membrane, where it induced membrane permeabilization. Then, TRP channels modulated intracellular Ca^{2+} rise that was necessary for transforming growth factor β-activated kinase 1 (TAK1) activation. This mechanism showed that low intracellular K^+ is required but not sufficient to induce activation of the NLRP3

Please cite this article in press as: Compan et al., Cell Volume Regulation Modulates NLRP3 Inflammasome Activation, Immunity (2012), http://dx.doi.org/10.1016/j.immuni.2012.06.013

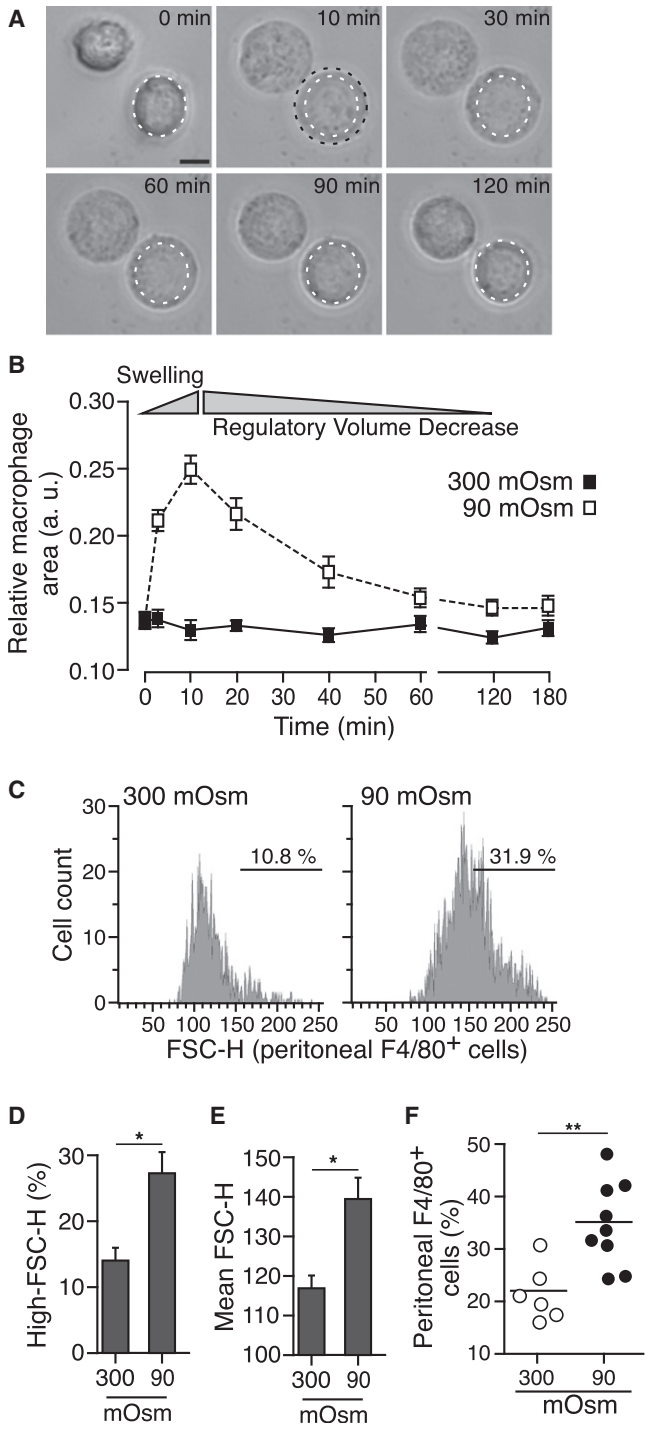

Figure 1. Hypotonic Solutions Are Considered Danger Signals In Vivo

(A) Time-lapse images of THP-1 cells in a hypotonic solution (90 mOsm), initial volume (white dotted line) and maximum volume (black dotted line) are indicated; scale bar represents 5 μm.

(B) Relative cell area of THP-1 cells in isotonic (continuous trace) or hypotonic (dotted trace) solution. n = 50 cells per condition; representative of four independent experiments. a.u., arbitrary units.

(C) Representative flow-cytometry forward scatter (FSC-H) plots of mouse F4/80 positive cells in the peritoneum of mice injected for 4 days with an iso- or hypotonic solution.

(D and E) Percentage of high-FSC-H (D) and mean-FCS-H (E) gated F4/80 positive peritoneal cells, as shown in (C). n = 3 animals per condition.

(F) Percentage of F4/80 positive cells in the peritoneum of mice injected for 4 days with an iso- (n = 6 animals, white circles) or hypotonic (n = 9 animals, black circles) solution.

Data are presented as mean ± SEM. $^{**}p < 0.005$; $^{*}p < 0.05$. See also Figure S1.

inflammasome. Our study gives a molecular target for the currently used hypertonic fluid therapy and shows that modulation of interstitial osmolarity and TRP inhibition could be beneficial for controlling inflammatory diseases involving the NLRP3 inflammasome.

RESULTS

Macrophage Swelling Activates Caspase-1 and IL-1β Release via the NLRP3 Inflammasome

We examined cell volume regulation of macrophages after exposure to changes in extracellular osmolarity. Human THP-1 macrophages responded to a reduction in extracellular osmolarity with cell swelling followed by an RVD process to recover their original cellular size (Figures 1A and 1B). Conversely, an increase in extracellular osmolarity induced macrophage shrinking followed by a regulatory-volume-increase response (Figure S1A available online). We made similar observations among different types of mononuclear and other nonimmune cells (Figures S1A–S1C). Recurrent sterile intraperitoneal (i.p) administration of hypotonic solution in mice induced macrophage swelling in vivo (Figures 1C–1E) and was sufficient to significantly increase the number of macrophages in the peritoneum compared with isotonic-solution-injected animals (Figure 1F).

After in vitro lipopolysaccharide (LPS) priming, a wide range of primary and immortalized human and murine macrophages responded to reduced extracellular osmolarity by releasing caspase-1-dependent cytokines IL-18 and IL-1β (Figures 2A, 2B, and S2A). Such release was not observed when cells were exposed to hypertonic solutions or for tumor necrosis factor-α (TNF-α), a caspase-1-independent cytokine (Figure 2A). The release of IL-1β was abolished with a specific caspase-1 inhibitor (Figure 2C). Active caspase-1 appeared in discrete isolated structures (Figure 2D), suggesting the presence of functional inflammasome-like particles. Contrary to the findings with classical caspase-1 activators (ATP, nigericin, MSU crystals, or aluminum [Alu]), a hypotonic solution was able to activate caspase-1 in both mammalian and teleost fish (*Sparus aurata*) macrophages (Figure 2E), both of which are sensitive to the NLRP3 blocker Bay11-7085 (Juliana et al., 2010) (Figures S2B and S2C).

In macrophages derived from mice deficient in caspase-1, ASC, or NLRP3, IL-1β release following hypotonicity was abolished (Figures 2F, S2D, and S2E) without affecting the RVD response (Figure S2F). In HEK293 cells, expression of NLRP3 inflammasome components demonstrated a requirement for ASC and the pyrin and NACHT domains of NLRP3 to activate caspase-1 in response to hypotonic stimulation, as well as to the K^+ ionophore nigericin, a classical NLRP3 activator (Figures 2G and S2G).

Please cite this article in press as: Compan et al., Cell Volume Regulation Modulates NLRP3 Inflammasome Activation, Immunity (2012), http://dx.doi.org/10.1016/j.immuni.2012.06.013

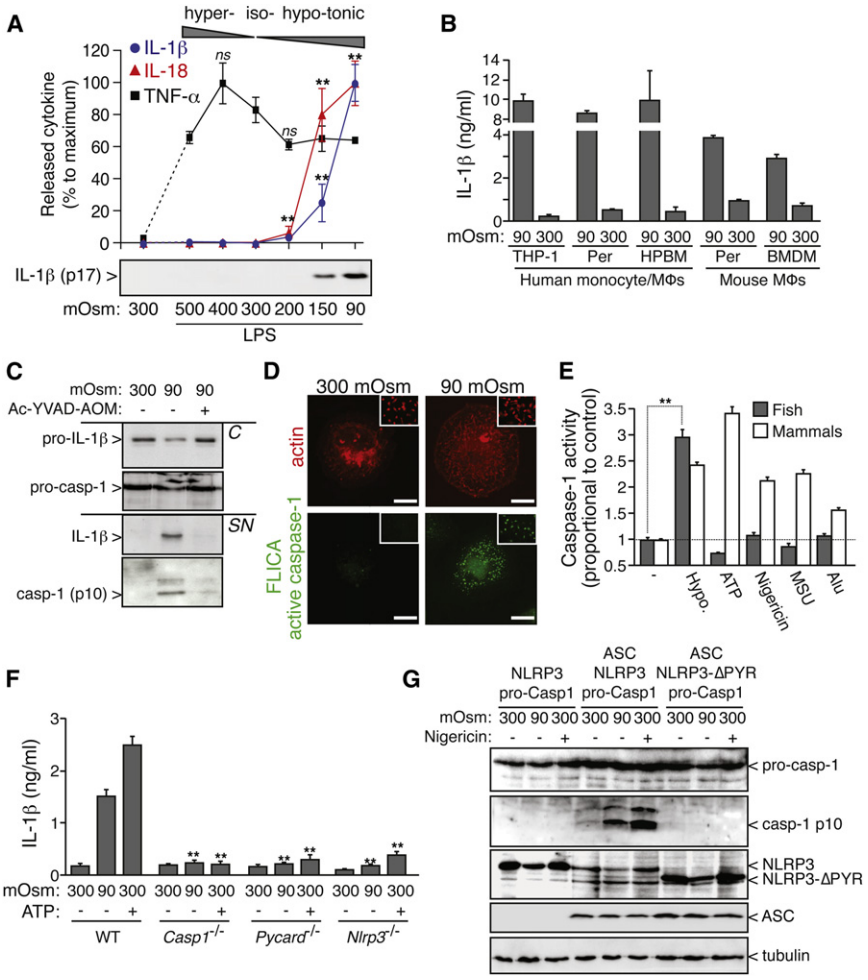

Figure 2. Macrophage Swelling Induces Release of IL-1β and Activation of Caspase-1 via the NLRP3 Inflammasome

(A) ELISA of released IL-1β (blue trace), IL-18 (red trace), or TNF-α (black trace) and western blot analysis of mature IL-1β released by THP-1 cells, primed or not with LPS (1 μg/ml, 4 hr), and subsequently subjected to different extracellular osmolarities for 1 hr; *ns*, no significant difference compared with isotonic conditions. n = 3 independent experiments. Maximum concentrations of IL-1β, IL-18, and TNF-α were 12.5 ± 0.58, 1.94 ± 0.11, and 1.49 ± 0.19 ng/ml, respectively.

(B) ELISA of IL-1β release by different macrophages (Mϕs) treated as described in (A). Human macrophages were: THP-1 cells, primary peritoneal macrophages (Per) and peripheral blood monocytes (HPBM); and mouse macrophages were: primary peritoneal macrophages (Per) and BMDM. n = 3–7 independent experiments.

(C) Western blot analysis of the cleavage of pro-IL-1β to its active p17 form (IL-1β) and of caspase-1 to its active p10 subunit by THP-1 cells treated as described in (A), in the presence or absence of the caspase-1 inhibitor (Ac-YVAD-AOM, 100 μM). *C*, cell lysates; *SN*, supernatants.

(D) Representative high-resolution, deconvolved images of mouse peritoneal macrophages treated as described in (A), stained with fluorescent probe for active caspase-1 (FLICA, green), and F-actin cytoskeleton stained with Texas red-phalloidin (red). Scale bar represents 2.5 μm. The inserts show staining of a population of >15 cells.

(E) Caspase-1 activity measured in fish macrophages (gray bars) or mouse BMDM (white bars) after hypotonic media stimulation (Hypo, 1 hr), ATP (5 mM, 30 min), nigericin (1 μM, 30 min mammalian and 1 hr fish), MSU crystals (500 μg/ml, 1 hr), or Alu crystals (500 μg/ml mammalian and 40 μg/ml fish, 1 hr). n = 3–4 independent experiments.

(F) ELISA of IL-1β release by bone marrow-derived wild-type (WT), caspase-1-deficient (*Casp1*$^{-/-}$), ASC-deficient (*Pycard*$^{-/-}$), or NLRP3-deficient (*Nlrp3*$^{-/-}$) macrophages treated as described in (A) or with 3 mM ATP for 30 min; n = 3 independent cultures.

(G) Western blot analysis of the cleavage of pro-caspase-1 to its active p10 subunit in HEK293 cells transfected with pro-caspase-1 and NLRP3; pro-caspase-1, NLRP3, and ASC; or pro-caspase-1, NLRP3-PYR deletion, and ASC, incubated for 1 hr with hypotonic solution or 30 min with nigericin (5 μM).

Data are presented as mean ± SEM. **p < 0.001. See also Figure S2.

Macrophage Swelling Activates NLRP3 Preassembled Complexes

To examine real-time intermolecular interactions between NLRP3 proteins during cell swelling, we labeled the terminus (C terminus: Ct; N terminus: Nt) of these proteins with yellow fluorescent protein (YFP) or Renilla-luciferase (Luc) to record bioluminescence resonance energy transfer (BRET) (Figure 3A). We first demonstrated that our NLRP3-YFP- and NLRP3-Luc-tagged proteins were still functional and were able to activate caspase-1 (Figure S3A). Using our validated model of swelling-induced inflammasome activation in HEK293 cells (Figures 2G and S1C), we found that prior to stimulation, NLRP3 proteins were in spatial proximity to each other, as a specific saturated BRET signal was found between them (Figure 3B). As a control, the noninteracting protein β-arrestin-YFP yielded a nonspecific linear increase of the BRET signal with NLRP3-Luc-Ct (Figure 3B). The BRET signal was higher between NLRP3-Luc-Ct and NLRP3-YFP-Nt than between NLRP3-Luc-Ct and NLRP3-YFP-Ct (Figure 3B), suggesting that in resting NLRP3 complexes, the pyrin-Nt of one NLRP3 protein is in closer proximity to the Ct of adjacent NLRP3 (see the proposed model in Figure 3J). Given that NLRP3 oligomerization is thought to occur through interaction between central NACHT domains (Schroder and Tschopp, 2010) and deletion of NACHT impairs caspase-1 activation after hypotonic stimulation (Figure S2G), BRET experiments were next performed with NLRP3 constructs deleted for this domain (NLRP3-ΔNACHT). When coexpressed with NLRP3-Luc-Ct, NLRP3-ΔNACHT-YFP-Ct yielded a nonspecific linear increase of the BRET signal (Figure S3B), confirming the role of NACHT domains in NLRP3 proteins' interaction and the specificity of the BRET signal among full-length NLRP3 molecules. Coexpression of ASC with NLRP3 induced an increase of the BRET signal between NLRP3 complexes (Figure 3C). NLRP3 protein interaction was further characterized with biochemical experiments. NLRP3-YFP and NLRP3-Flag proteins coimmunoprecipitated (coIP) under both resting conditions

Please cite this article in press as: Compan et al., Cell Volume Regulation Modulates NLRP3 Inflammasome Activation, Immunity (2012), http://dx.doi.org/10.1016/j.immuni.2012.06.013

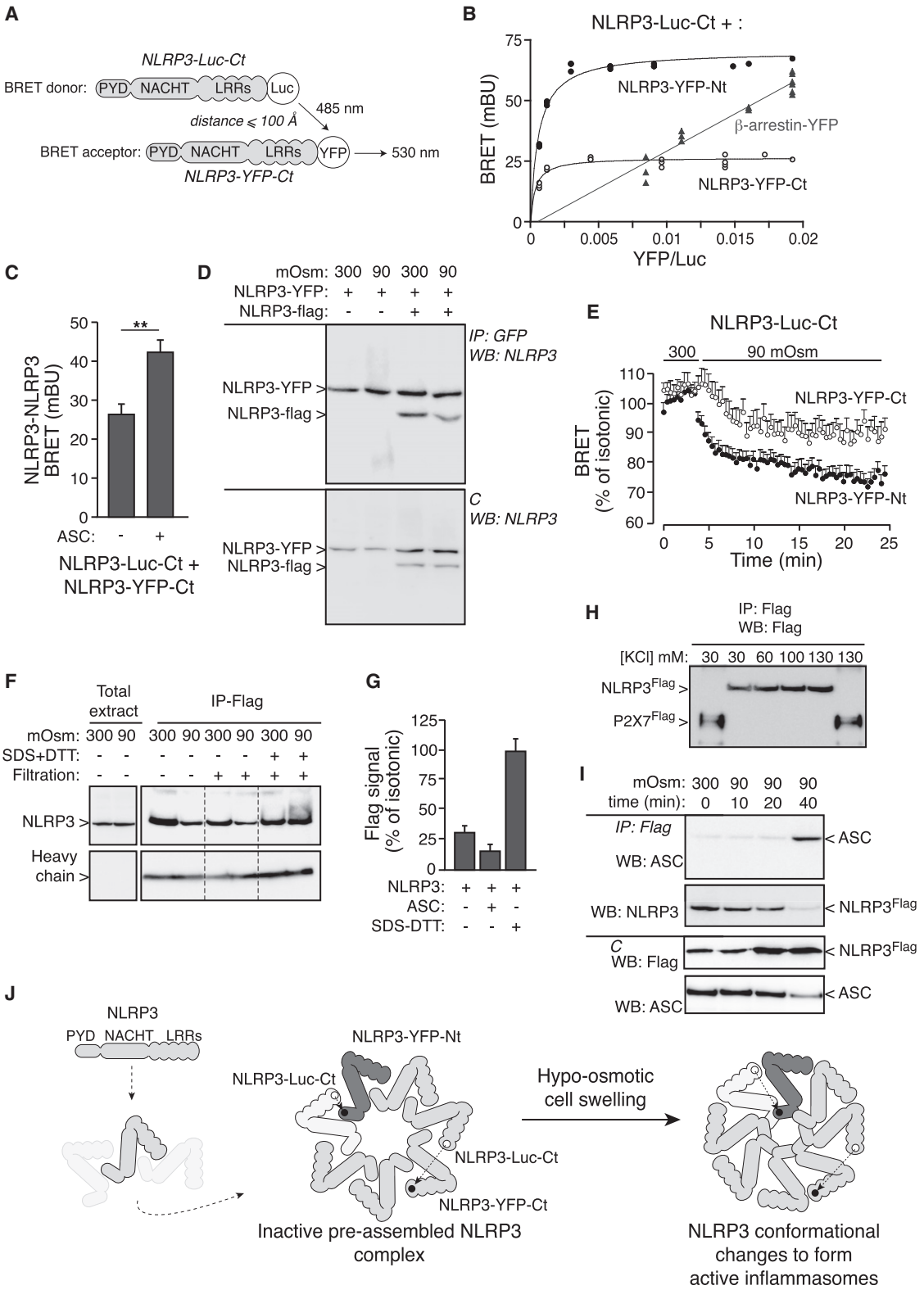

Figure 3. NLRP3 Proteins Form an Inactive Preassembled Complex in Resting Cells

(A) Schematic representation showing NLRP3 BRET donor and acceptor partners.

(B) BRET saturation curves for HEK293 cells transfected with a constant concentration of NLRP3-Luc-Ct and increasing amounts of the BRET acceptor NLRP3-YFP-Nt (black circles), NLRP3-YFP-Ct (open circles), or β-arrestin-YFP (gray triangles). mBU, milliBRET units.

(C) BRET signal from HEK293 cells transfected with NLRP3-Luc-Ct and NLRP3-YFP-Ct in the presence or absence of ASC coexpression; **$p < 0.001$.

and after a decrease in extracellular osmolarity (Figure 3D), showing that NLRP3 protein interactions were not affected by the stimulation. NLRP3 oligomerization was highly reduced when the NACHT domain of NLRP3 was deleted (Figure S3C).

During the first 5 min after hypotonic stimulation, the magnitude of the BRET signal between NLRP3 proteins was reduced (Figure 3E). This reduction was more pronounced between NLRP3-Luc-Ct and NLRP3-YFP-Nt (Figure 3E) and was absent if cells were maintained in isotonic conditions (Figure S3D). In control samples, we observed no change in the BRET signal after hypotonic stimulation using a Luc-YFP fusion construct (Figure S3E). The decrease in BRET signal observed for NLRP3 proteins during hypotonic shock was also found after nigericin treatment (Figure S3F) and was due to a conformational change in the proteins rather than a dissociation of NLRP3-NLRP3 complexes, because we found similar coIP among NLRP3 proteins before and after hypotonic stimulation (see Figure 3D). Conformational changes in NLRP3 proteins were further confirmed by studying the Flag-tagged immunoprecipitation (Flag IP) efficiency of NLRP3-Flag-Nt proteins. Indeed, fewer proteins were pulled down after a hypotonic stimulation (Figures 3F and 3G), without any degradation or release of NLRP3 proteins (Figures S3G and S3H). The NLRP3 IP efficiency was restored when either NLRP3 proteins were denatured before being pulled down (Figures 3F and3G) or when high K^+ concentrations were used during the IP (Figure 3H). As a control, purinergic receptor P2X, ligand-gated ion channel, 7 (P2X7)-Flag IP was not affected by the different K^+ concentrations (Figure 3H). This suggests a K^+-dependent conformational change of NLRP3 after hypotonic stimulation, which could alter the accessibility of the antibody to the Flag epitope. The reduced IP efficiency was more prominent with ASC coexpression (Figure 3G), supporting the idea that ASC is able to compact the Nt of the NLRP3 inflammasome by interacting with its pyrin domain. Despite the evidence of ASC interaction with inactive NLRP3 complexes (Figures 3C and 3G), direct protein interaction between NLRP3 and ASC was only evident in coIP experiments after 40 min in hypotonic solution (Figure 3I).

Potassium Depletion Is Not Sufficient to Activate the NLRP3 Inflammasome

We first found that activation of caspase-1 induced by hypotonicity was dependent on intracellular K^+ efflux (Figures 4A–4C), as this is an established and obligatory step for activating the NLRP3 inflammasome (Schroder and Tschopp, 2010). It is known that cell swelling activates Cl^- efflux in conjunction with K^+ loss to initiate cellular water efflux and maintain cellular homeostasis via RVD (Hoffmann et al., 2009). As expected, macrophage intracellular K^+ concentration decreased during the first 10 min of cell swelling (Figure 4A). Blocking intracellular K^+ depletion by using a hypotonic solution with a high concentration of K^+ and glycerol (a membrane-permeable molecule that maintains hypotonicity) still induced cell swelling but abolished the RVD response and the release of mature IL-1β (Figures 4B and 4C), suggesting that in addition to K^+ efflux, RVD could be an important process in activating the inflammasome. To further investigate the role of RVD in the activation of the inflammasome, we studied the decrease of intracellular Cl^- as a controlling step for the RVD (Figures 4D and 4E). Using NPPB, a general blocker of swelling-activated Cl^- channels, we found that preventing the RVD response also inhibited the release of mature IL-1β (Figures 4E and 4F). Interestingly, NPPB did not alter the depletion of intracellular K^+ mediated by cell swelling (Figure 4G). Thus, intracellular K^+ depletion per se is necessary but not sufficient to induce swelling-evoked processing and release of IL-1β.

TRP Channels Regulate Caspase-1 Activation

We found that in response to hypotonic stimulation, macrophages became permeable for large fluorescent molecular tracer (Figures 5A and S4A). This dye uptake occurred during RVD (after 10 min of stimulation) and was not dependent on pannexin-1, P2X7 receptor, or caspase-1 activation (Figures S4B and S4C). We were able to rule out the possible actions of ATP released during cell permeabilization activating the NLRP3 inflammasome, because neither macrophages deficient in P2X7 receptors nor treatment with apyrase (an enzyme that degrades ATP) affected IL-1β release in response to hypotonicity (Figures S4D and S4E). Treatment with the cathepsin B inhibitor Ca-047-Me did not impair caspase-1 activation or IL-1β release in response to hypotonicity; therefore, we also ruled out the involvement of cathepsin B in inflammasome activation (Figures S4G–S4I); however, hypotonicity was able to induce lysosome destabilization, as measured by cathepsin release (Figure S4F). Hypotonicity-induced dye uptake was sensitive to broad TRP channel blockers (Figure 5A), and TRP inhibition strongly suppressed hypotonicity-induced caspase-1 activation and IL-1β release without affecting K^+ efflux in both mammalian and fish macrophages (Figures 5B, 5C, S4J, and S4K). We analyzed the expression of TRP channels in macrophages and found expression of eight different subunits, TRPV2 and TRPM7 being the ones most expressed (Figure 5D). TRPV2 has been previously identified as an osmosensor, and TRPM7 has been involved in controlling the RVD process (Liedtke, 2006; Muraki et al., 2003; Numata et al., 2007). Blocking TRPM7 function by using high extracellular Mg^{2+} concentration (Penner and Fleig, 2007) delayed macrophage RVD, decreased cell

(D) NLRP3-YFP and NLRP3-Flag coIP in resting conditions or after hypotonic stimulation in HEK293 cells (*C*: cell lysates). Western blots are representative of three independent experiments.

(E) Kinetics of net BRET signal in HEK293 cells transfected with the BRET donor NLRP3-Luc-Ct and the acceptor NLRP3-YFP-Nt (black circles) or NLRP3-YFP-Ct (open circles) in response to hypotonic solution.

(F–H) NLRP3-Flag or P2X7-Flag IP after hypotonic stimulation in HEK293. IP was performed on naive or denatured (SDS + dithiothreitol [DTT]) lysates (F) and in the presence of different concentrations of K^+ (H). Histograms in (G) are the densitometry quantification of the NLRP3-Flag IP signal after hypotonic stimulation of three independent blots in the absence or the presence of ASC cotransfection.

(I) Kinetics of coIP between ASC and NLRP3-Flag in HEK293 cells after hypotonic stimulation; *C*, total cell lysates. Western blots are representative of two to three independent experiments.

(J) Proposed model for the intermolecular dynamics of NLRP3 inflammasome activation in response to hypotonicity.

Data are presented as mean ± SEM. See also Figure S3.

Please cite this article in press as: Compan et al., Cell Volume Regulation Modulates NLRP3 Inflammasome Activation, Immunity (2012), http://dx.doi.org/10.1016/j.immuni.2012.06.013

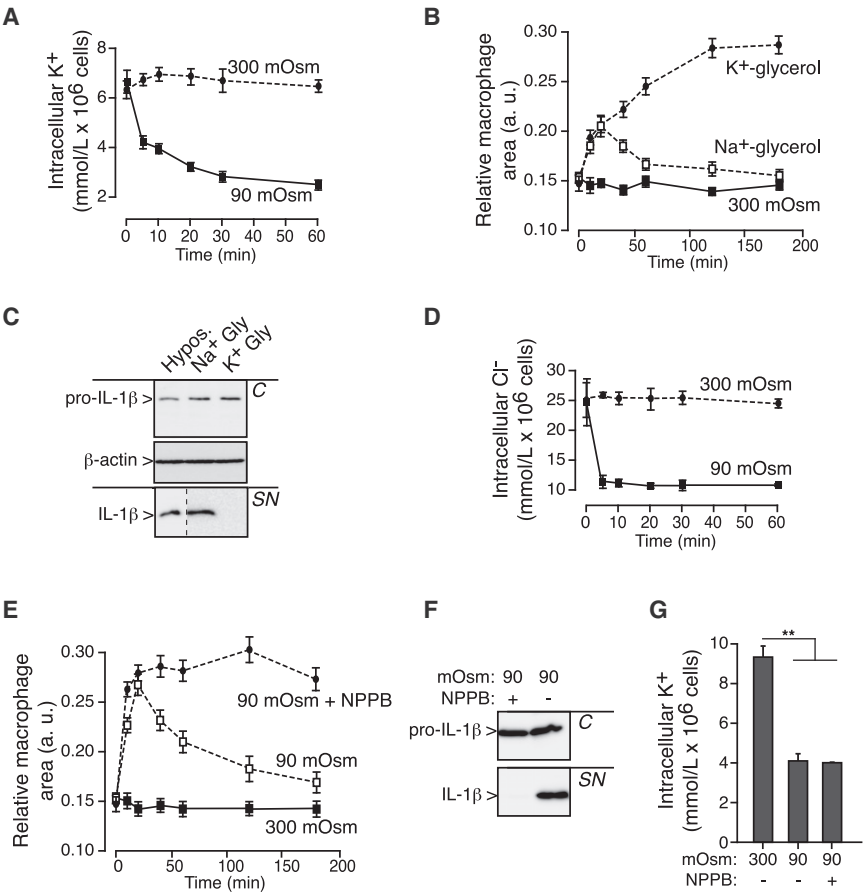

Figure 4. RVD Controls Activation of the NLRP3 Inflammasome

(A) Relative intracellular K^+ concentration of THP-1 cells primed with LPS (1 μg/ml, 4 hr) and subsequently subjected to 300 or 90 mOsm extracellular solution for 1 hr; n = 3 independent experiments.

(B) Relative cell area of THP-1 cells in isotonic solution (continuous trace) or in hypotonic solutions composed of 120 mM glycerol (dotted trace) and either 140 mM of NaCl (open squares) or 140 mM of KCl (black circles). n = 50 cells per treatment; representative of three independent experiments. a.u., arbitrary units.

(C) Western blot analysis of β-actin and of the cleavage of pro-IL-1β to its active p17 form (IL-1β) by LPS-primed THP-1 cells incubated for 1 hr with a 90 mOsm hypotonic solution (Hypos.) or in hypotonic solutions composed of 120 mM glycerol and either 140 mM NaCl (Na^+ Gly) or 140 mM of KCl (K^+ Gly). *C*, cell lysates; *SN*, supernatants.

(D) Relative intracellular Cl^- concentration of THP-1 cells treated as in (A); n = 3 independent experiments.

(E) Relative cell area of THP-1 cells in isotonic solution (continuous trace) or in 90 mOsm solution (dotted line) in the absence (open squares) or presence (closed circles) of 100 μM NPPB. n = 50 cells per treatment; representative of three independent experiments. a.u., arbitrary units.

(F) Western blot analysis of the cleavage of pro-IL-1β to its active p17 form (IL-1β) on THP-1 cells treated as in (A) in the presence or absence of NPPB (100 μM).

(G) Relative intracellular K^+ concentration of THP-1 cells treated as in (A) in the presence or absence of NPPB (100 μM).

Western blots are representative of two to three independent experiments. Data are presented as mean ± SEM. **p < 0.001.

permeabilization, and reduced the release of IL-1β (Figures 5E–5G). Similar results were obtained using the broad TRP channel blockers lanthanum, ruthenium red, and 2-APB (Figures 5A, 5C, S4J, and S4O). Alternatively, it is known that the absence of extracellular Mg^{2+} potentiates TRPM7 function (Penner and Fleig, 2007), and we found that in macrophages exposed to hypotonic solution, the absence of Mg^{2+} accelerated RVD and increased cell permeabilization and IL-1β release (Figures 5E–5G). Due to the lack of selective antagonists, TRPV2 involvement was studied after silencing in THP-1 using small hairpin RNA (shRNA) (Figures S4L and S4M). TRPV2 gene silencing decreased the dye uptake and the release of IL-1β in response to hypotonic treatment (Figures 5H and 5I) without affecting the RVD (Figure S4N). As previously described (Nagasawa et al., 2007), we found that macrophage TRPV2 channels were localized on intracellular endosomes (Figure 5J) and were translocated to the plasma membrane after hypotonic stimulation (Figure 5K).

TRP Activation Modulates Intracellular Ca^{2+} and TAK1 Phosphorylation

TRP are cationic channels permeable to Ca^{2+}. BAPTA-AM treatment of THP-1 cells completely abolished the processing and release of IL-1β in response to hypotonicity (Figure 6A), and intracellular Ca^{2+} variation during cell volume regulation was sensitive to 2-APB (Figure 6B). It has been shown that membrane stretch and intracellular Ca^{2+} activate TAK1 and that this kinase plays a role in NLRP3 inflammasome activation (Fukuno et al., 2011; Gong et al., 2010). We found that a decrease in extracellular osmolarity induced phosphorylation of TAK1 (Figure 6C), which is required for TAK1 activation (Sakurai et al., 2000). Specific inhibition of TAK1 phosphorylation with the use of 5Z-7-oxozeaenol blocked hypotonicity-induced caspase-1 activation and IL-1β processing in a dose-dependent manner (Figure 6C) without affecting intracellular K^+ depletion (Figure 6D) or the RVD (Figure 6E). Activation of TAK1 was abolished in the presence of BAPTA-AM (Figure 6C) or when RVD was blocked using NPPB (Figure 6F). Meanwhile, TRP channel inhibitor 2-APB blocked TAK1 phosphorylation (Figure 6G). IL-1β release induced by hypotonicity was also highly reduced in cells wherein the TAK1 gene was silenced (Figure 6H). Altogether, these results show that during hypotonic stimulation, TAK1 plays a key signaling role downstream of TRP channels in the activation of the NLRP3 inflammasome.

Hypertonic Solutions and TRP Inhibition Prevent the Activation of the Inflammasome

Because a decrease in extracellular osmolarity induced NLRP3 activation, we next determined whether cell volume regulation

might be a general mechanism for controlling the NLRP3 inflammasome. Using an in vivo model of ear inflammation dependent on NLRP3 inflammasome activation (Sutterwala et al., 2006; Watanabe et al., 2007) (Figures 7A and 7B), we found that the size of macrophages was enlarged within the inflamed tissue (Figures 7C and 7D). The in vivo use of 2-APB decreased both ear inflammation and macrophage size (Figures 7A–7D), suggesting the importance of macrophage size and TRP function during inflammation as a feature of cell activation. Also, treatment of macrophages in vitro with 2-APB or La^{3+} blocked IL-1β release induced by classical NLRP3 inflammasome activators, such as nigericin, *Escherichia coli*, or MSU crystals (Figure 7E). Such treatments did not affect IL-1β release induced by DNA-mediated AIM2 inflammasome activation (Figure 7E).

As expected, increasing media osmolarity in vitro with NaCl, mannitol, or sorbitol inhibited hypotonicity-induced IL-1β release (Figures 7F and 7G). We also found that hypertonic solutions suppressed NLRP3 inflammasome-dependent IL-1β release induced by nigericin, *E. coli*, Alu, and MSU crystals (Figures 7F and 7G), without affecting AIM2 inflammasome activation (Figure 7G). Hypertonic solutions did not alter K^+ efflux after nigericin treatment (Figure S5B), suggesting that such solutions do not work by affecting K^+ efflux. However, cell swelling and RVD were not common features of inflammasome activation; for example, nigericin treatment induced a decrease in intracellular K^+ concentration and cell shrinking without affecting intracellular Cl^- concentration (Figures S5A and S5C). Macrophages were viable in iso-, hypo-, and hypertonic solutions, and gene expression for NLRP3, ASC, and caspase-1 was not affected by these treatments (Figures S5D and S5E).

We wanted to confirm the in vivo relevance of this finding and determine the molecular bases for the current use of hypertonic solutions in clinics during brain inflammation (Jain, 2008). We first found that a hypotonic solution activated caspase-1 in mouse hippocampal neurons in culture (Figure 7H), confirming previous data on functional neuronal caspase-1 (de Rivero Vaccari et al., 2008). As a proof of concept, we used a rat brain-injury model induced by injection of kainic acid into the hippocampus to induce cell swelling in vivo (Oprica et al., 2003). Microdialysis perfusion of kainic acid in the hippocampus mainly activated caspase-1 in the neurons of the pyramidal layer and dentate gyrus (Figure 7I) and promoted the release of IL-1β (Figure 7J). Both effects, caspase-1 activation and IL-1β release, were reduced by perfusing a 20% sorbitol hypertonic solution after the administration of kainic acid (Figures 7I and 7J).

Altogether, our data identify cell volume regulation as a basic conserved homeostatic mechanism associated with the formation and stimulation of the NLRP3 inflammasome via TRP channels sensing cell swelling and controlling TAK1 activation.

DISCUSSION

In this study, we found that, among vertebrates, macrophage swelling induced by hypotonic solutions is a conserved danger signal for activating the NLRP3 inflammasome. This process was dependent on the decrease of intracellular K^+ and Cl^- and a correct RVD process controlled by TRP channels. However, it acted independently of P2X7 receptor signaling and cathepsin B. As already described for other NLRP3 activators, K^+ depletion was a necessary step to induce the activation of the inflammasome. Nevertheless, our study points out that this ionic depletion is not sufficient to induce caspase-1 activation after hypotonicity or nigericin treatment. We also provided molecular mechanistic insights into the assembly and activation of the NLRP3 inflammasome in real time. Finally, our data showed that an increase in extracellular osmolarity abrogated, in vivo, caspase-1 activation induced by cell swelling in immune (macrophages) and nonimmune (neurons) cells.

Cell volume regulation is an ancient protection mechanism for a change in extracellular osmolarity. During evolution, this cellular response has been adapted as a signaling pathway involved in many pathophysiological processes (Hoffmann et al., 2009). We found that low osmolarity solutions and cell swelling induced the recruitment of macrophages in vivo and could be considered as a potential danger signal recognized by the immune system. In fact, cell swelling was strongly associated with the activation of macrophages within the inflamed tissue, with caspase-1 activation, and with the release of IL-1β and IL-18 through the NLRP3 inflammasome. Lower vertebrates and invertebrates present an expanded family of NLR receptors (Hansen et al., 2011), but their function in controlling innate immunity is not well understood, given that in fish and other lower vertebrates, IL-1β sequence lacks a clear caspase-1 processing site (López-Castejón et al., 2008; Pelegrín et al., 2004). In measuring caspase-1 activation, we found that contrary to ATP, nigericin, MSU crystals, or Alu, a hypotonic solution was able to activate caspase-1 in both mammalian and fish macrophages. This result identifies hypotonic environments as an evolutionary alert mechanism conserved from fish to mammalian macrophages for activating caspase-1.

The present model for NLRP3 inflammasome activation is that upon activation, NLRP3 proteins oligomerize and thereby interact with ASC to form a functional multiprotein complex that activates caspase-1 (Jha and Ting, 2009; Schroder and Tschopp, 2010). We used the BRET technique to study inflammasome protein dynamics in real time. Before any stimulation, NLRP3 proteins formed a preassembled complex, as already described for the NLRP1 inflammasome (Faustin et al., 2007). In this complex, the pyrin domain of one NLRP3 was in close proximity to the LRR domain of an adjacent NLRP3. Self-oligomerization of NLRP3 seems to be mediated by interaction of the NACHT domains, in that the BRET signal and coIP were impaired for NACHT-deleted NLRP3 constructs. ASC was able to interact through the pyrin domain and compact preassembled NLRP3 resting complexes, similar to what happened during inflammasome activation.

The NLRP3 inflammasome senses a wide range of danger signals, including extracellular ATP or MSU crystals (Mariathasan et al., 2006; Martinon et al., 2006); however, there is no clear common mechanism of NLRP3 activation. Our results demonstrate that a common step is probably membrane stretch, which induces activation of channels (like TRPV2 or pannexin-1) that permeabilize cell membranes (Pelegrín and Surprenant, 2006, 2007). All known activators of the NLRP3 inflammasome induce cell volume changes (swelling or shrinking) (Dise et al., 1980; Schorn et al., 2011; Taylor et al., 2008), and the NLRP3 inflammasome could be a sensor of cellular membrane integrity. Upon hypotonic cell swelling, the decrease in intracellular

Please cite this article in press as: Compan et al., Cell Volume Regulation Modulates NLRP3 Inflammasome Activation, Immunity (2012), http://dx.doi.org/10.1016/j.immuni.2012.06.013

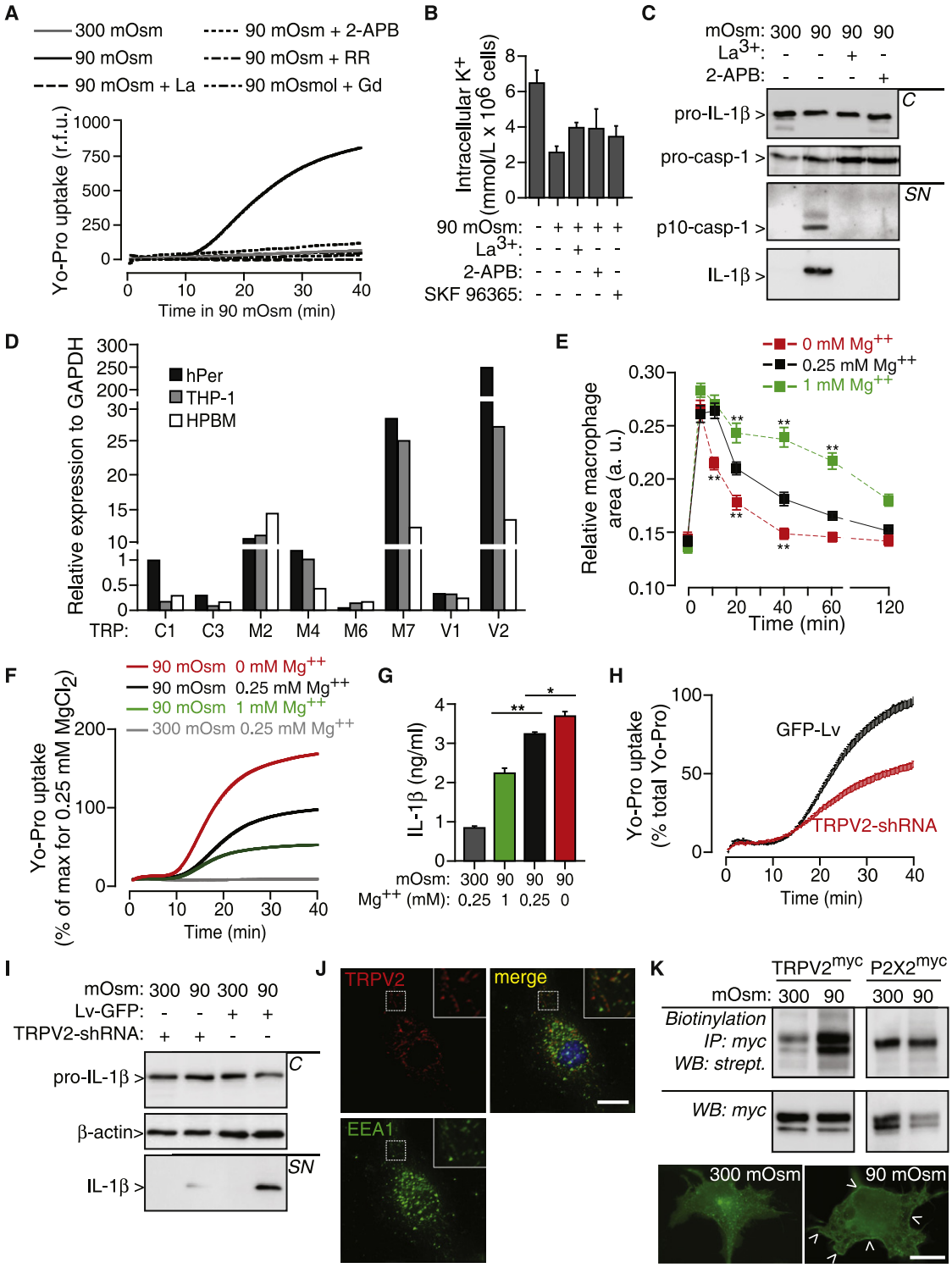

Figure 5. TRP Channels Control Caspase-1 Activation During RVD

(A) Kinetics of Yo-Pro uptake in THP-1 cells during hypotonicity in the absence or presence of $LaCl_3$ (La, 2 mM), 2-APB (100 μM), ruthenium red (RR, 100 μM), or $GdCl_3$ (Gd, 2 mM); average traces of three independent experiments. r.f.u., relative fluorescence units.

(B) Relative intracellular K^+ concentration of THP-1 cells treated as described in (A); n = 3 independent experiments.

(C) Western blot analysis of the cleavage of pro-IL-1β to its active p17 form (IL-1β) and of caspase-1 to its active p10 subunit by THP-1 cells treated as described in (A). *C*, cell lysates; *SN*, supernatants.

(D) qRT-PCR of TRP channel family expression in THP-1 cells, human peritoneal macrophages (hPer), and blood monocytes (HPBM).

(E) Relative cell area of THP-1 cells in 90 mOsm solution with different concentrations of Mg^{2+}. a.u., arbitrary units.

K^+ concentration carried by activation of mechanosensitive potassium channels favored a conformational change in NLRP3 proteins by generating the appropriate intracellular environment for inflammasome activation, probably by increasing electrostatic interactions between NLRP3 proteins as already proposed (Zhang et al., 2011). However, our results rule out intracellular K^+ depletion as the unique cause of caspase-1 activation, because blocking RVD with Cl^- or TRP channel inhibitors abolished the release of mature IL-1β without altering cellular K^+ depletion. Moreover, this conclusion was extended to other NLRP3 activators, because IL-1β release induced by nigericin was completely blocked by hypertonic solution without affecting K^+ efflux. Both K^+ and Cl^- depletion activated RVD in macrophages as a protection mechanism for elevated membrane tension. Therefore, extracellular osmolarity was sensed by macrophages as a danger signal due to the increase in cellular membrane tension during cell swelling, rather than only a depletion of intracellular K^+ or a direct detection of a change in extracellular ionic strength. Indeed, swelling induced by glycerol in a sodium solution of normal extracellular ionic strength still induced caspase-1 activation. RVD is controlled by the activation of different membrane channels, including TRPM7 (Numata et al., 2007). We found that, following cell swelling, a TRP channel with a pharmacology profile similar to TRPM7 (sensitive to ruthenium red, lanthanum, gadolinium, 2-APB, and magnesium concentration) regulated RVD in macrophages. After maximum stretch during cell swelling, endomembranes derived from endosomes and lysosomes are used to repair plasma membrane damages (Togo et al., 2000). In macrophages, we observed that this endomembrane fusion during RVD induced TRPV2 trafficking to the cell surface. As already described for large organic cations, TRPV2 activation is responsible for membrane permeabilization to large molecules (Banke et al., 2010). General blockers of TRP channels abolished RVD (probably controlled by TRPM7), cell permeabilization (due to TRPV2), and caspase-1 activation without altering intracellular K^+ depletion. Cell permeabilization during swelling is also related to the release of cytosolic ATP (Boudreault and Grygorczyk, 2004), which prompts autocrine and/or paracrine purinergic P2X7 receptor signaling and NLRP3 inflammasome activation (Babelova et al., 2009; Iyer et al., 2009; Sanz et al., 2009; Weber et al., 2010). Also, P2X7-induced IL-1β release has been attributed to cell swelling (Perregaux et al., 1996). However, under hypotonic conditions, swelling-induced ATP release and P2X7 receptor stimulation were not involved in the activation of NLRP3. Our data show that TRP channel activation modulates intracellular Ca^{2+} during cell volume regulation, and this change in intracellular calcium appears to be crucial for the activation of TAK1. A recent study has revealed that TAK1 plays a key role in NLRP3 inflammasome activation (Gong et al., 2010) and that TAK1 might be activated by intracellular Ca^{2+} variations after membrane stretch (Fukuno et al., 2011). We found that, following hypotonic stimulation, TAK1 activation was regulated by TRP activity during RVD and was required for caspase-1 activation and IL-1β processing. We also found that TRP blockers were effective in inhibiting MSU crystal- and nigericin-induced caspase-1 activation, but the specific involvement of TRP channels, particularly of TRPV2, in NLRP3 activation will have to be confirmed by genetic ablation in mouse models (Link et al., 2010).

Hypertonic solutions are used in clinics to reduce brain edema and to reconstitute fluids in patients with trauma or severe sepsis (Jain, 2008; Oliveira et al., 2002). We found that macrophages at inflamed tissues present a characteristic morphology with a considerable increase in cellular volume, sensitive to TRP blockers. In vitro, hypertonic solutions were able to inhibit the NLRP3 inflammasome in response to different stimuli without affecting IL-1β release induced by AIM2 activation. These results suggest that cellular volume changes specifically modulate activation of the NLRP3 inflammasome toward other inflammatory supramolecular complexes. Although the different NLRP3 stimuli do not directly cause cell swelling (Dise et al., 1980; Taylor et al., 2008), the potential benefit of inhibiting inflammasome activation by inducing cell shrinking using hypertonic solution reinforces the current clinical use of hypertonic osmotherapy to treat different inflammatory diseases (Jain, 2008; Oliveira et al., 2002). To date, the beneficial anti-inflammatory effects of hypertonic solutions have mainly been attributed to instantaneous hemodynamic redistribution of interstitial and cellular water into the circulation by the osmotic gradient produced (Diringer and Zazulia, 2004; Oliveira et al., 2002). However, their use for reducing inflammation is highly debated, given that no clear molecular mechanism has been attributed to their action. We found that, in vivo, kainic acid administration activates caspase-1 in neurons and IL-1β release. Perfusion of a hypertonic solution reduced both effects and demonstrates that neuronal cell swelling in vivo is also coupled with caspase-1 activation. Although NLRP1 has been proposed as the neuronal inflammasome platform (de Rivero Vaccari et al., 2008), it needs to be confirmed whether in vivo kainic acid activates the NLRP3 or NLRP1 inflammasome in neurons. These data support

(F) Kinetics of Yo-Pro uptake in THP-1 cells during hypotonic solution stimulation with different concentrations of Mg^{2+}; average traces of three independent experiments.

(G) ELISA of IL-1β released by THP-1 cells primed with LPS (1 μg/ml, 4 hr) and subsequently subjected to different extracellular osmolarities for 1 hr with different concentrations of Mg^{2+}; n = 6 independent experiments.

(H) Kinetics of Yo-Pro uptake in THP-1 cells infected with GFP-lentivirus (GFP-Lv) or with shTRPV2-lentivirus (TRPV2-shRNA) during hypotonic solution stimulation; average traces of three independent experiments.

(I) Western blot analysis of β-actin and of the cleavage of pro-IL-1β to its active p17 form (IL-1β) by THP-1 cells infected as described in (H). *C*, cell lysates; *SN*, supernatants.

(J) High-resolution, deconvolved images of TRPV2 and EEA1 immunostaining on mouse peritoneal macrophages; scale bar represents 2.5 μm.

(K) TRPV2-myc or P2X2-myc plasma membrane biotinylation (top panels), total cell lysate immunoblot (middle panels), or TRPV2-myc immunostaining (bottom panels) on HEK293 cells treated for 40 min with iso- or hypotonic solution. Scale bar represents 2.5 μm; arrowhead denotes TRPV2 membrane localization. strept., streptavidin-HRP.

Data are presented as mean ± SEM. *$p < 0.05$; **$p < 0.005$. See also Figure S4.

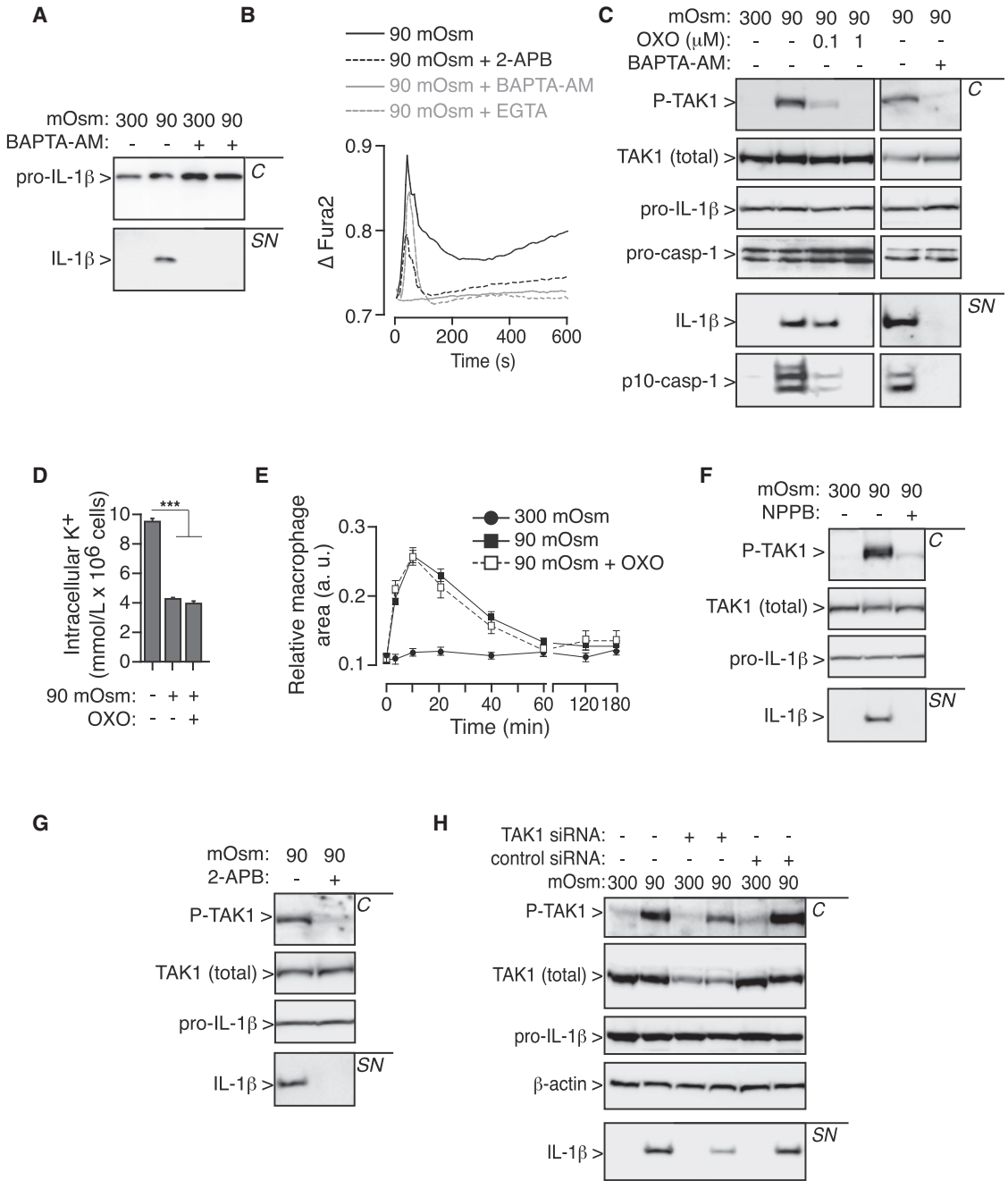

Figure 6. TRP Channels Modulate Macrophage Intracellular Ca^{2+} and TAK1 Activation

(A) Western blot analysis of the cleavage of pro-IL-1β to its active p17 form (IL-1β) by THP-1 cells primed with LPS (1 μg/ml, 4 hr) and subsequently subjected to 300 or 90 mOsm extracellular solution for 1 hr, in the presence or absence of BAPTA-AM (100 μM).

(B) Intracellular Ca^{2+} changes of THP-1 cells treated as in (A) in the presence or absence of 2-APB (100 μM), BAPTA-AM (100 μM), or an extracellular buffer without calcium (EGTA).

(C) Western blot analysis of TAK1 phosphorylation and the cleavage of pro-IL-1β to its active p17 form (IL-1β) and of caspase-1 to its active p10 subunit by THP-1 cells treated as in (A), in the presence or absence of different concentrations of 5Z-7-oxozeaenol (OXO) or BAPTA-AM (100 μM).

(D) Relative intracellular K^+ concentration of THP-1 cells primed as in (C); n = 3 independent experiments.

(E) Relative cell area of THP-1 cells treated as in (C). n = 50 cells per condition. a.u., arbitrary units.

(F and G) Western blot analysis of TAK1 phosphorylation and the cleavage of pro-IL-1β to its active p17 form (IL-1β) by THP-1 cells treated as in (A), in the presence or absence of NPPB (100 μM) (F), or 2-APB (100 μM) (G).

(H) Western blot analysis of TAK1 phosphorylation, β-actin, and the cleavage of pro-IL-1β to its active p17 form (IL-1β) by THP-1 cells silenced or not for the TAK1 gene, following hypotonic stimulation.

Data are presented as mean ± SEM.

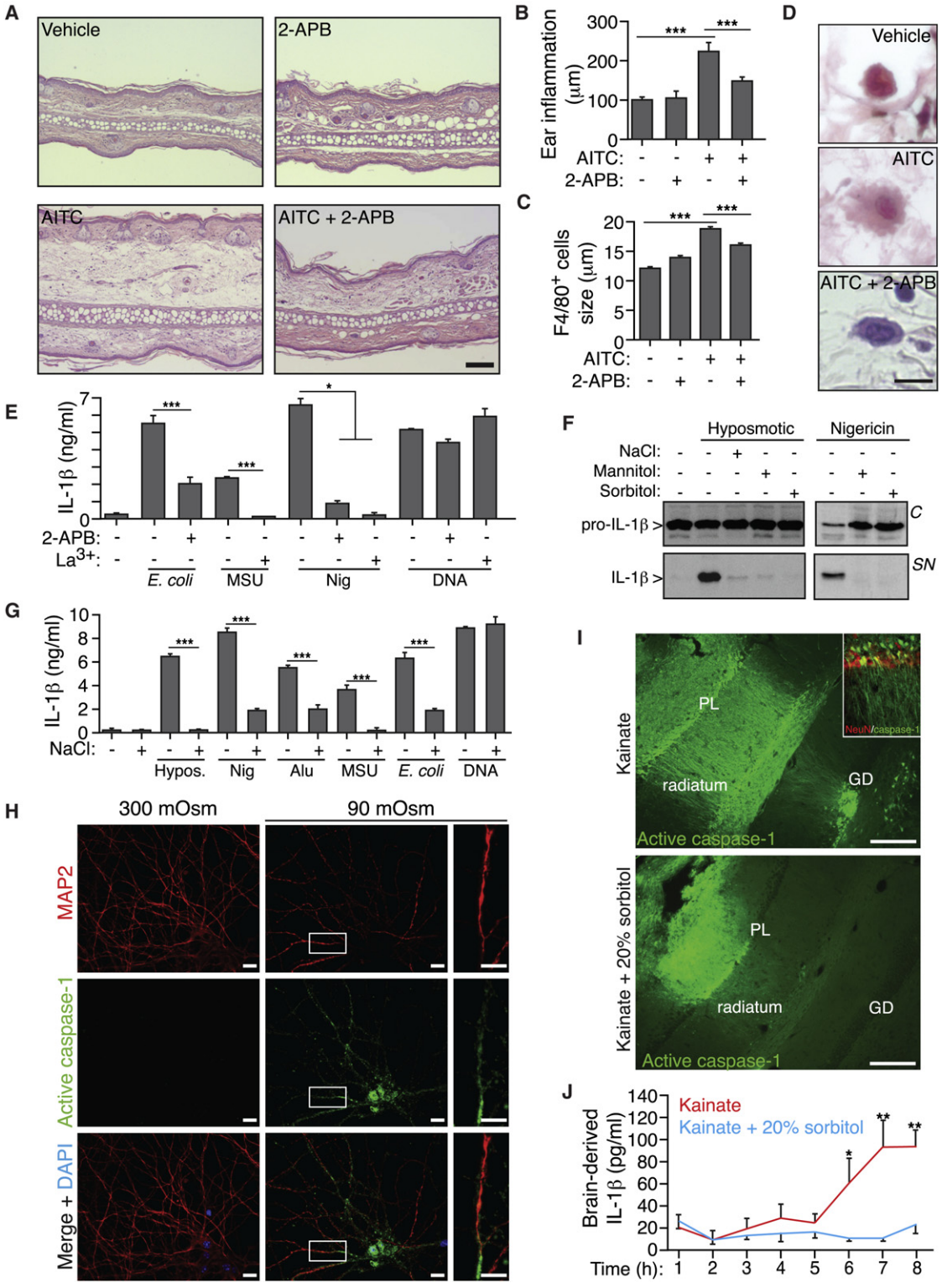

Figure 7. Inflammation Is Blocked by TRP Inhibition or Hypertonic Solutions

(A) Representative histology of mouse ear inflammatory model induced with allyl isothiocyanate (AITC) in the presence of absence of 2-APB (100 μM); representative of five different animals; scale bar represents 40 μm.

(B) Measurements of ear inflammation (n = 25 sections per condition).

(C) Measurements of F4/80 positive macrophage size inside the inflamed ear tissue (n = 30–60 macrophages per condition).

(D) Representative histology of mouse ear macrophage; scale bar represents 20 μm.

previous studies indicating that the activation of caspase-1 could contribute to the proinflammatory effects associated with different brain pathologies, such as epilepsy or stroke, wherein neuronal swelling has been reported (de Rivero Vaccari et al., 2008; Rothwell, 2003; Simard et al., 2007).

Altogether, these results reveal that drugs targeting TRP channels or the signaling pathway of cell volume regulatory process are promising tools for reduction of inflammation, as well as for treatment of pathologies linked to caspase-1 and NLRP3 activation. Therefore, we propose cell swelling as an evolutionarily conserved homeostatic mechanism associated with the formation of the NLRP3 inflammasome.

EXPERIMENTAL PROCEDURES

Animals

Male C57BL/6 mice (6–8 weeks old) were obtained from Harlan and maintained in specific pathogen-free conditions. Healthy specimens (150 g) of the marine fish gilt-head sea bream (*Sparus aurata*, Actinopterygii, Sparidae) were maintained in 14 m^3 running seawater aquaria. The local ethical committees from University Hospital Virgen de la Arrixaca, University of Murcia, and Hospital Ramón y Cajal approved all animal experiments. *P2rx7*-deficient mice (Chessell et al., 2005) were from the laboratory of A. Verkhratsky, and bone marrow from *Casp1*- (Kuida et al., 1995), *Nlrp3*- (Martinon et al., 2006), and *Pycard*- (Mariathasan et al., 2004) deficient mice were a generous gift of I. Coullin.

Intraperitoneal Administration of Hypotonic Solution

Mice were treated with daily i.p. injections of 100 ml/kg^1 of iso- or hypotonic solution for 4 consecutive days. Three hours after the last injection, animals were sacrificed, and peritoneal cavities were washed. The lavage was analyzed for macrophage size and presence by flow cytometry using F4/80-AlexaFluor488 antibody (Caltag) on a FACScalibur (BD Biosciences). The macrophage population was analyzed using WinList software (Verity Software House).

Kainic Acid Brain Injury Model

Brain microdialysis of kainic acid in adult Sprague-Dawley rats aged 10–12 weeks was already described (Hsu et al., 2007; Oprica et al., 2003). In brief, each hippocampus was stereotaxically (anterior-posterior: −4.6 mm; lateral: ± 2.6 mm from bregma; ventral: 2.6 mm from dura) implanted with a CMA/12 microdialysis probe (CMA Microdialysis); after 2 hr washout, 100 μM kainic acid was perfused for 1 hr (flow: 1 μl/min), followed by the infusion of isotonic Krebs-Ringer bicarbonate (KRB) solution (280–290 mOsm) in one hippocampus and hypertonic KRB supplemented with 20% sorbitol (1400–1500 mOsm) in the contralateral side. Samples for IL-1β analysis were collected every hour for 8 hr. At the end of the experiment, the biotinylated caspase-1 inhibitor (100 μm biotinyl-YVAD-CMK, AnaSpec) was perfused for 1 hr. After 12 hr, animals were sacrificed, and brains were removed for immunohistochemical studies.

Cells, Treatments, and Procedures

Mouse primary bone marrow-derived macrophages (BMDM), peritoneal macrophages, immortalized mouse BMDM, fish macrophages, and THP-1 and HEK293 cell cultures were described previously (Hornung et al., 2008; López-Castejón et al., 2008; Lopez-Castejon et al., 2010; Pelegrín and Surprenant, 2009). For details of hippocampal cultures, human macrophage isolation, and BRET measurements, see Supplemental Information. If not specified, all macrophages were primed for 4 hr with LPS (1 μg/ml) previous to hypotonic-solution challenge. For TRPV2 gene silencing, THP-1 cells were infected with recombinant lentivirus vectors, and experiments were performed 7 days after infection. For TAK1 gene silencing, THP-1 cells were cultured in the presence of an *Accell* TAK1 small interfering RNA (siRNA) or *Accell* nontargeting siRNA pool (Thermo Scientific Dharmacon) for 72 hr according to manufacturer's instruction. If not mentioned in the text, all the hypo- and isotonic solutions had an osmolarity of 90 and 300 mOsm, respectively. The 90 mOsm hypotonic solution was achieved by diluting isotonic physiology electrophysiology-total buffer (Pelegrín and Surprenant, 2009) 1:4 with distilled sterile water.

Detailed methods for quantitative RT-PCR (qRT-PCR), RT-PCR, immunocytochemistry, microscopy, western blots, coIP, IP, lactate dehydrogenase measurements, ELISA, cathepsin release, dye uptake, plasma membrane biotynilation, and FLICA (fluorescent labeled inhibitor of caspases) staining have been previously described (López-Castejón et al., 2008; Lopez-Castejon et al., 2010; Pelegrín and Surprenant, 2009). Intracellular K^+ concentration was analyzed on a Hitachi-917 (Roche). Macrophage area measurements were quantified from >50 cells per condition per time point using National Institutes of Health (NIH) ImageJ software (http://rsb.info.nih.gov/ij). The University Hospital Virgen de la Arrixaca clinical ethics committee approved the collection of human samples, upon patient consent, for purifying human peritoneal macrophages and peripheral blood monocytes.

Statistical Analysis

All data are shown as mean values, and error bars represent SEM from the number of assays indicated (from at least three independent experiments). For statistical comparisons, data were analyzed by an unpaired two-tailed Student's t test to determine differences between groups using Prism software (GraphPad Software); the p value is indicated in the figure legends.

SUPPLEMENTAL INFORMATION

Supplemental Information includes five figures and Supplemental Experimental Procedures and can be found with this article online at http://dx.doi.org/10.1016/j.immuni.2012.06.013.

ACKNOWLEDGMENTS

We thank I. Couillin for *Casp1*-, *Pycard*-, and *Nlrp3*-deficient mice bone marrow, A. Verkhratsky for *P2rx7* receptor-deficient mice, E. Latz for immortalized BMDM from C57BL/6 and *Pycard*- and *Nlrp3*-deficient mice, and F. Rassendren for TRPV2-shRNA lentivirus. We thank J. Tschopp for NLRP3-Flag, G. Dubyak for ASC-V5, J. Perroy for Luc-YFP, and J.P. Pin for β-arrestin-YFP expression vectors. We thank O. Fernandez for advice with animal models, L. Martinez-Alarcón for human blood extraction, F. Machado-Linde for collecting human peritoneal lavages, F. Noguera for running Hitachi ion detection system, P.J. Martínez for animal handling, E. Moutin for hippocampal neuron culture, and E. Martin, R. Gaskell, I. Fuentes, and M.C. Baños for both molecular and cellular technical assistance. We would like to thank A. Surprenant and F. Rassendren for helpful

(E–G) IL-1β release detected by ELISA (E and G) or western blot (F) in THP-1 cells primed for 4 hr with LPS (1 μg/ml) and treated with hypotonic solution (90 mOsm, Hypos. or Hyposmotic), nigericin (25 μM, Nig), Alu (500 mg/ml), MSU (500 mg/ml), *E. coli* challenge, or lipofectamine-DNA complexes (DNA). Where indicated, the buffer was supplemented with 2-APB (100 μM), $LaCl_3$ (La, 2 mM), NaCl (150 mM), sorbitol (20%), or mannitol (20%). n = 3–4 independent experiments.

(H) Representative images of hippocampal mouse neurons in culture, treated with a hypotonic solution for 30 min and stained with fluorescent probe for active caspase-1 (FLICA, green), MAP2 (red), and DAPI. Scale bars represent 20 μm (left and middle panels) and 10 μm (right panels).

(I) Histochemical detection of active caspase-1 in the rat hippocampus after administration of 100 μM kainate in isotonic or hypertonic solution (Krebs-Ringer bicarbonate solution supplemented with 20% of sorbitol). Active caspase-1 (green) colocalizes with NeuN-positive neurons (insert, red) of the pyramidal layer (PL) and the dentate gyrus (GD). Scale bar represents 100 μm.

(J) ELISA of IL-1β release in the hippocampus of rats after administration of 100 μM kainate in iso- (red trace) or hyper- (blue trace) tonic solution; n = 4 animals per treatment.

Data are presented as mean ± SEM. ***p < 0.001; **p < 0.005; *p < 0.05. See also Figure S5.

discussions and support. We are indebted to R.A. North, D. Brough, L.E. Browne, and O. Stelmashenko for critical revision of the manuscript. V.C. is supported by a grant from the Wellcome Trust. This work was supported by grants from Plan Nacional de Investigación Científica, Desarrollo, e Innovación Tecnológica 2008–2011 (PN de I+D+I 2008–2011), Instituto de Salud Carlos III, and Fondo Europeo de Desarrollo Regional (FEDER) (EMER07/049 and PI09/0120); Fundación Séneca (11922/PI/09), managed by Fundación para la Formación e Investigación Sanitarias de la Región de Murcia (FFIS); and grants from the Spanish Ministry of Science and Technology (BIO2008-01379 and BIO2011-23400) and Fundación Marcelino Botín.

Received: July 26, 2011
Revised: April 30, 2012
Accepted: June 7, 2012
Published online: September 13, 2012

REFERENCES

Babelova, A., Moreth, K., Tsalastra-Greul, W., Zeng-Brouwers, J., Eickelberg, O., Young, M.F., Bruckner, P., Pfeilschifter, J., Schaefer, R.M., Gröne, H.-J., and Schaefer, L. (2009). Biglycan, a danger signal that activates the NLRP3 inflammasome via toll-like and P2X receptors. J. Biol. Chem. *284*, 24035–24048.

Banke, T.G., Chaplan, S.R., and Wickenden, A.D. (2010). Dynamic changes in the TRPA1 selectivity filter lead to progressive but reversible pore dilation. Am. J. Physiol. Cell Physiol. *298*, C1457–C1468.

Boudreault, F., and Grygorczyk, R. (2004). Cell swelling-induced ATP release is tightly dependent on intracellular calcium elevations. J. Physiol. *561*, 499–513.

Chessell, I.P., Hatcher, J.P., Bountra, C., Michel, A.D., Hughes, J.P., Green, P., Egerton, J., Murfin, M., Richardson, J., Peck, W.L., et al. (2005). Disruption of the P2X7 purinoceptor gene abolishes chronic inflammatory and neuropathic pain. Pain *114*, 386–396.

de Rivero Vaccari, J.P., Lotocki, G., Marcillo, A.E., Dietrich, W.D., and Keane, R.W. (2008). A molecular platform in neurons regulates inflammation after spinal cord injury. J. Neurosci. *28*, 3404–3414.

Diringer, M.N., and Zazulia, A.R. (2004). Osmotic therapy: fact and fiction. Neurocrit. Care *1*, 219–233.

Dise, C.A., Goodman, D.B., and Rasmussen, H. (1980). Selective stimulation of erythrocyte membrane phospholipid fatty acid turnover associated with decreased cell volume. J. Biol. Chem. *255*, 5201–5207.

Faustin, B., Lartigue, L., Bruey, J.-M., Luciano, F., Sergienko, E., Bailly-Maitre, B., Volkmann, N., Hanein, D., Rouiller, I., and Reed, J.C. (2007). Reconstituted NALP1 inflammasome reveals two-step mechanism of caspase-1 activation. Mol. Cell *25*, 713–724.

Feldmeyer, L., Keller, M., Niklaus, G., Hohl, D., Werner, S., and Beer, H.-D. (2007). The inflammasome mediates UVB-induced activation and secretion of interleukin-1beta by keratinocytes. Curr. Biol. *17*, 1140–1145.

Fukuno, N., Matsui, H., Kanda, Y., Suzuki, O., Matsumoto, K., Sasaki, K., Kobayashi, T., and Tamura, S. (2011). TGF-β-activated kinase 1 mediates mechanical stress-induced IL-6 expression in osteoblasts. Biochem. Biophys. Res. Commun. *408*, 202–207.

Gong, Y.-N., Wang, X., Wang, J., Yang, Z., Li, S., Yang, J., Liu, L., Lei, X., and Shao, F. (2010). Chemical probing reveals insights into the signaling mechanism of inflammasome activation. Cell Res. *20*, 1289–1305.

Hansen, J.D., Vojtech, L.N., and Laing, K.J. (2011). Sensing disease and danger: a survey of vertebrate PRRs and their origins. Dev. Comp. Immunol. *35*, 886–897.

Hoffmann, E.K., Lambert, I.H., and Pedersen, S.F. (2009). Physiology of cell volume regulation in vertebrates. Physiol. Rev. *89*, 193–277.

Hornung, V., Bauernfeind, F., Halle, A., Samstad, E.O., Kono, H., Rock, K.L., Fitzgerald, K.A., and Latz, E. (2008). Silica crystals and aluminum salts activate the NALP3 inflammasome through phagosomal destabilization. Nat. Immunol. *9*, 847–856.

Hsu, Y.H., Lee, W.T., and Chang, C. (2007). Multiparametric MRI evaluation of kainic acid-induced neuronal activation in rat hippocampus. Brain *130*, 3124–3134.

Iyer, S.S., Pulskens, W.P., Sadler, J.J., Butter, L.M., Teske, G.J., Ulland, T.K., Eisenbarth, S.C., Florquin, S., Flavell, R.A., Leemans, J.C., and Sutterwala, F.S. (2009). Necrotic cells trigger a sterile inflammatory response through the Nlrp3 inflammasome. Proc. Natl. Acad. Sci. USA *106*, 20388–20393.

Jain, K.K. (2008). Neuroprotection in traumatic brain injury. Drug Discov. Today *13*, 1082–1089.

Jha, S., and Ting, J.P. (2009). Inflammasome-associated nucleotide-binding domain, leucine-rich repeat proteins and inflammatory diseases. J. Immunol. *183*, 7623–7629.

Juliana, C., Fernandes-Alnemri, T., Wu, J., Datta, P., Solorzano, L., Yu, J.-W., Meng, R., Quong, A.A., Latz, E., Scott, C.P., and Alnemri, E.S. (2010). Anti-inflammatory compounds parthenolide and Bay 11-7082 are direct inhibitors of the inflammasome. J. Biol. Chem. *285*, 9792–9802.

Kuida, K., Lippke, J.A., Ku, G., Harding, M.W., Livingston, D.J., Su, M.S., and Flavell, R.A. (1995). Altered cytokine export and apoptosis in mice deficient in interleukin-1 beta converting enzyme. Science *267*, 2000–2003.

Lang, F., Busch, G.L., Ritter, M., Völkl, H., Waldegger, S., Gulbins, E., and Häussinger, D. (1998). Functional significance of cell volume regulatory mechanisms. Physiol. Rev. *78*, 247–306.

Li, G., Bauer, S., Nowak, M., Norwood, B., Tackenberg, B., Rosenow, F., Knake, S., Oertel, W.H., and Hamer, H.M. (2011). Cytokines and epilepsy. Seizure *20*, 249–256.

Liedtke, W. (2006). Transient receptor potential vanilloid channels functioning in transduction of osmotic stimuli. J. Endocrinol. *191*, 515–523.

Link, T.M., Park, U., Vonakis, B.M., Raben, D.M., Soloski, M.J., and Caterina, M.J. (2010). TRPV2 has a pivotal role in macrophage particle binding and phagocytosis. Nat. Immunol. *11*, 232–239.

López-Castejón, G., Sepulcre, M.P., Mulero, I., Pelegrín, P., Meseguer, J., and Mulero, V. (2008). Molecular and functional characterization of gilthead seabream Sparus aurata caspase-1: the first identification of an inflammatory caspase in fish. Mol. Immunol. *45*, 49–57.

Lopez-Castejon, G., Theaker, J., Pelegrín, P., Clifton, A.D., Braddock, M., and Surprenant, A. (2010). P2X(7) receptor-mediated release of cathepsins from macrophages is a cytokine-independent mechanism potentially involved in joint diseases. J. Immunol. *185*, 2611–2619.

Mariathasan, S., Newton, K., Monack, D.M., Vucic, D., French, D.M., Lee, W.P., Roose-Girma, M., Erickson, S., and Dixit, V.M. (2004). Differential activation of the inflammasome by caspase-1 adaptors ASC and Ipaf. Nature *430*, 213–218.

Mariathasan, S., Weiss, D.S., Newton, K., McBride, J., O'Rourke, K., Roose-Girma, M., Lee, W.P., Weinrauch, Y., Monack, D.M., and Dixit, V.M. (2006). Cryopyrin activates the inflammasome in response to toxins and ATP. Nature *440*, 228–232.

Martinon, F., Pétrilli, V., Mayor, A., Tardivel, A., and Tschopp, J. (2006). Gout-associated uric acid crystals activate the NALP3 inflammasome. Nature *440*, 237–241.

Muraki, K., Iwata, Y., Katanosaka, Y., Ito, T., Ohya, S., Shigekawa, M., and Imaizumi, Y. (2003). TRPV2 is a component of osmotically sensitive cation channels in murine aortic myocytes. Circ. Res. *93*, 829–838.

Nagasawa, M., Nakagawa, Y., Tanaka, S., and Kojima, I. (2007). Chemotactic peptide fMetLeuPhe induces translocation of the TRPV2 channel in macrophages. J. Cell. Physiol. *210*, 692–702.

Newman, P.J., and Grana, W.A. (1988). The changes in human synovial fluid osmolality associated with traumatic or mechanical abnormalities of the knee. Arthroscopy *4*, 179–181.

Numata, T., Shimizu, T., and Okada, Y. (2007). TRPM7 is a stretch- and swelling-activated cation channel involved in volume regulation in human epithelial cells. Am. J. Physiol. Cell Physiol. *292*, C460–C467.

Oliveira, R.P., Velasco, I., Soriano, F.G., and Friedman, G. (2002). Clinical review: Hypertonic saline resuscitation in sepsis. Crit. Care *6*, 418–423.

Oprica, M., Eriksson, C., and Schultzberg, M. (2003). Inflammatory mechanisms associated with brain damage induced by kainic acid with special reference to the interleukin-1 system. J. Cell. Mol. Med. *7*, 127–140.

Pelegrín, P., and Surprenant, A. (2006). Pannexin-1 mediates large pore formation and interleukin-1beta release by the ATP-gated P2X7 receptor. EMBO J. *25*, 5071–5082.

Pelegrín, P., and Surprenant, A. (2007). Pannexin-1 couples to maitotoxin- and nigericin-induced interleukin-1beta release through a dye uptake-independent pathway. J. Biol. Chem. *282*, 2386–2394.

Pelegrín, P., and Surprenant, A. (2009). Dynamics of macrophage polarization reveal new mechanism to inhibit IL-1beta release through pyrophosphates. EMBO J. *28*, 2114–2127.

Pelegrín, P., Chaves-Pozo, E., Mulero, V., and Meseguer, J. (2004). Production and mechanism of secretion of interleukin-1beta from the marine fish gilthead seabream. Dev. Comp. Immunol. *28*, 229–237.

Penner, R., and Fleig, A. (2007). The Mg2+ and Mg(2+)-nucleotide-regulated channel-kinase TRPM7. Handb. Exp. Pharmacol. *179*, 313–328.

Perregaux, D.G., Laliberte, R.E., and Gabel, C.A. (1996). Human monocyte interleukin-1beta posttranslational processing. Evidence of a volume-regulated response. J. Biol. Chem. *271*, 29830–29838.

Rothwell, N. (2003). Interleukin-1 and neuronal injury: mechanisms, modification, and therapeutic potential. Brain Behav. Immun. *17*, 152–157.

Sakurai, H., Miyoshi, H., Mizukami, J., and Sugita, T. (2000). Phosphorylation-dependent activation of TAK1 mitogen-activated protein kinase kinase kinase by TAB1. FEBS Lett. *474*, 141–145.

Sanz, J.M., Chiozzi, P., Ferrari, D., Colaianna, M., Idzko, M., Falzoni, S., Fellin, R., Trabace, L., and Di Virgilio, F. (2009). Activation of microglia by amyloid beta requires P2X7 receptor expression. J. Immunol. *182*, 4378–4385.

Schorn, C., Frey, B., Lauber, K., Janko, C., Strysio, M., Keppeler, H., Gaipl, U.S., Voll, R.E., Springer, E., Munoz, L.E., et al. (2011). Sodium overload and water influx activate the NALP3 inflammasome. J. Biol. Chem. *286*, 35–41.

Schroder, K., and Tschopp, J. (2010). The inflammasomes. Cell *140*, 821–832.

Simard, J.M., Kent, T.A., Chen, M., Tarasov, K.V., and Gerzanich, V. (2007). Brain oedema in focal ischaemia: molecular pathophysiology and theoretical implications. Lancet Neurol. *6*, 258–268.

Sutterwala, F.S., Ogura, Y., Szczepanik, M., Lara-Tejero, M., Lichtenberger, G.S., Grant, E.P., Bertin, J., Coyle, A.J., Galán, J.E., Askenase, P.W., and Flavell, R.A. (2006). Critical role for NALP3/CIAS1/Cryopyrin in innate and adaptive immunity through its regulation of caspase-1. Immunity *24*, 317–327.

Taylor, S.R.J., Gonzalez-Begne, M., Dewhurst, S., Chimini, G., Higgins, C.F., Melvin, J.E., and Elliott, J.I. (2008). Sequential shrinkage and swelling underlie P2X7-stimulated lymphocyte phosphatidylserine exposure and death. J. Immunol. *180*, 300–308.

Togo, T., Krasieva, T.B., and Steinhardt, R.A. (2000). A decrease in membrane tension precedes successful cell-membrane repair. Mol. Biol. Cell *11*, 4339–4346.

Watanabe, H., Gaide, O., Pétrilli, V., Martinon, F., Contassot, E., Roques, S., Kummer, J.A., Tschopp, J., and French, L.E. (2007). Activation of the IL-1beta-processing inflammasome is involved in contact hypersensitivity. J. Invest. Dermatol. *127*, 1956–1963.

Weber, F.C., Esser, P.R., Müller, T., Ganesan, J., Pellegatti, P., Simon, M.M., Zeiser, R., Idzko, M., Jakob, T., and Martin, S.F. (2010). Lack of the purinergic receptor P2X(7) results in resistance to contact hypersensitivity. J. Exp. Med. *207*, 2609–2619.

Zhang, Z., Witham, S., and Alexov, E. (2011). On the role of electrostatics in protein-protein interactions. Phys. Biol. *8*, 035001.

Zhou, R., Tardivel, A., Thorens, B., Choi, I., and Tschopp, J. (2010). Thioredoxin-interacting protein links oxidative stress to inflammasome activation. Nat. Immunol. *11*, 136–140.

Immunity, Volume *37*

Supplemental Data

Cell Volume Regulation Modulates NLRP3 Inflammasome Activation

Vincent Compan, Alberto Baroja-Mazo, Gloria López-Castejón, Ana I. Gomez, Carlos M. Martínez, Diego Angosto, María T. Montero, Antonio S. Herranz, Eulalia Bazán, Diana Reimers, Victoriano Mulero, and Pablo Pelegrín

Inventory of Supplemental Information

Supplemental Figures

Supplemental Experimental Procedures

Supplemental Acknowledgments

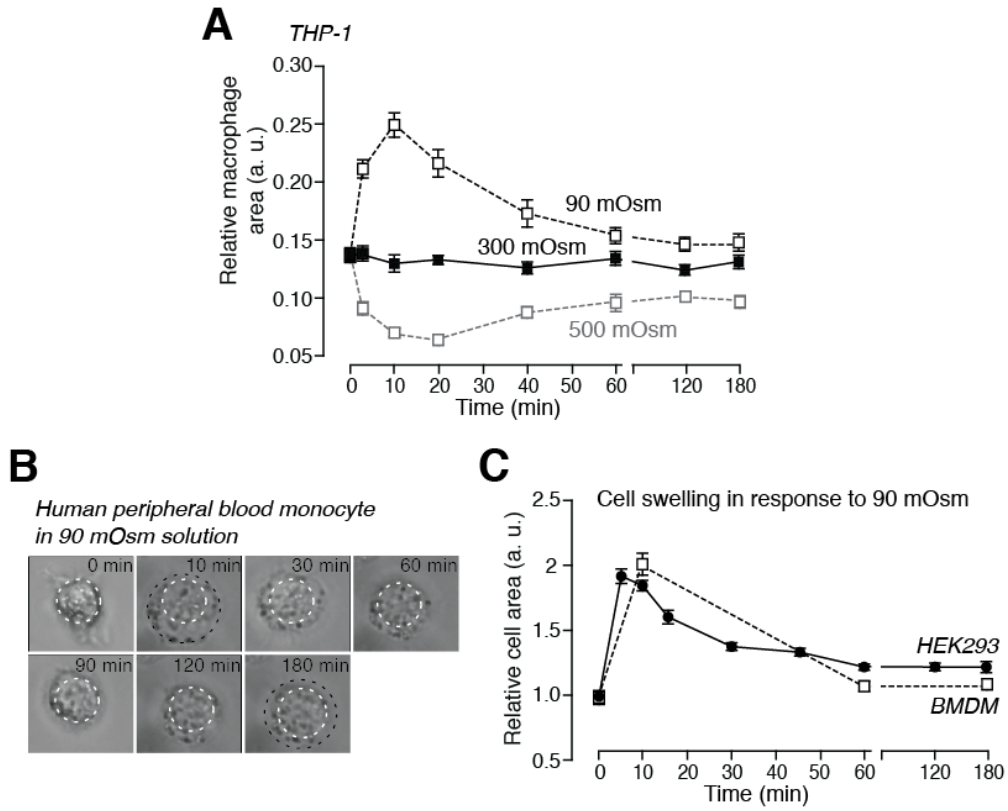

Figure S1. Hypotonicity Induces Macrophage Cell Swelling and IL-1β Release Relative cell area of THP-1 (**A**), human peripheral blood monocyte (**B**), immortalized BMDM (**C**, dotted line) or HEK293 cells (**C**, continuous line) exposed to different osmolarities as indicated. *n* = 60 to 50 cells per condition for A,C and representative monocyte pictures for B.

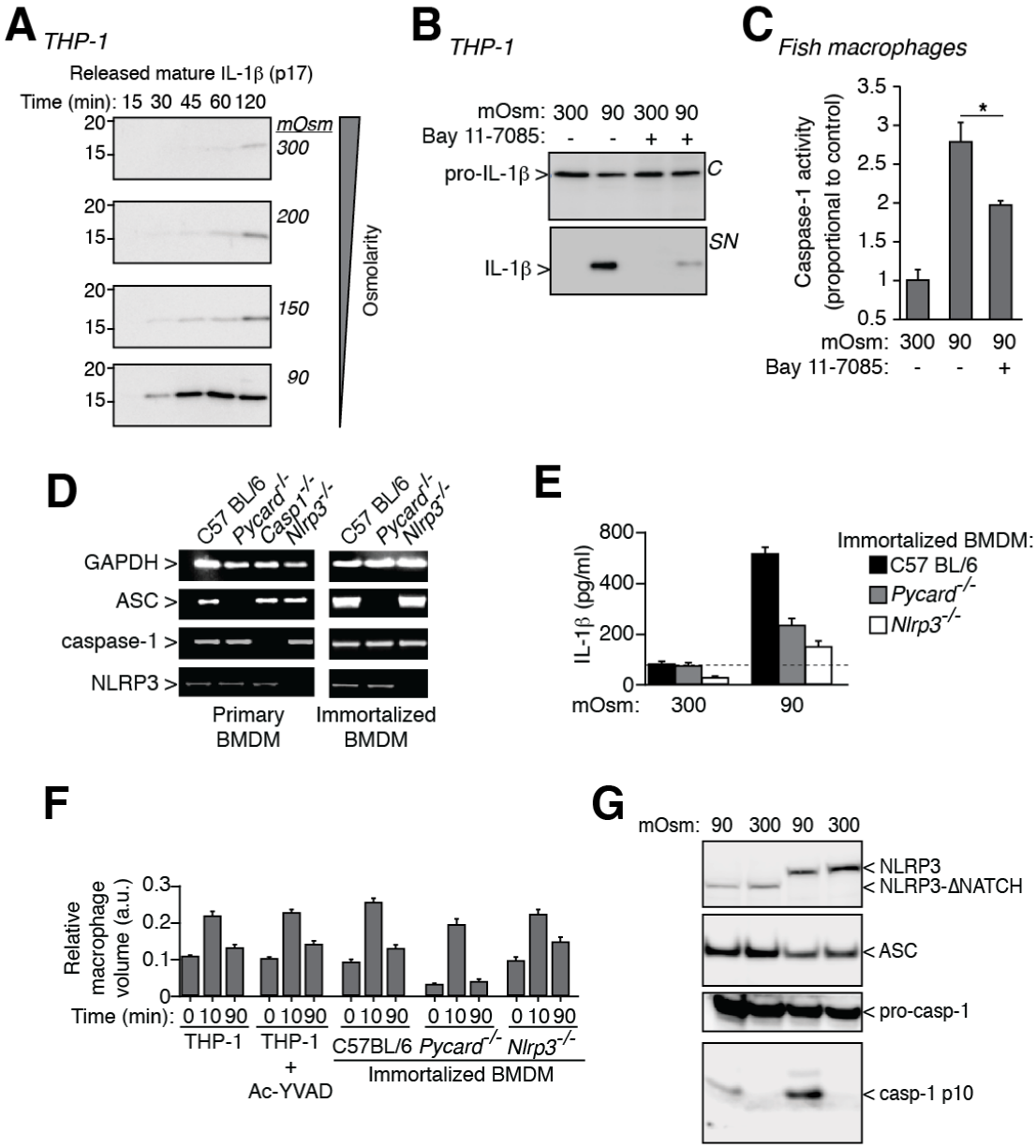

Figure S2. Hypotonic Solution Induces NLRP3 Inflammasome Activation
A,B, Western blot analysis of mature IL-1β release by THP-1 macrophages primed with LPS (4h, 1 μg/ml) and subsequent incubation during different times and

osmolarities (A) or 40 min in a hypotonic solution in the presence or absence of Bay 11-7085 (20 μM, 5 min before stimulation) (B); *C*: cell extracts, *SN*: supernatants; blots are representative of 3 independent experiments. **C,** Caspase-1 activity in fish macrophages induced by 1h of hypotonic solution in the presence or absence of Bay 11-7085 (20 μM, 10 min before stimulation); n = 3 to 9 independent experiments, *$p<0.05$. **D,** RT-PCR of GAPDH, ASC, caspase-1 and NLRP3 of immortalized BMDM from C57BL/6, *Pycard*$^{-/-}$ or *Nlrp3*$^{-/-}$ mice and primary BMDM from different genetically invalidated mice (*Pycard*$^{-/-}$, *Casp1*$^{-/-}$, *Nlrp3*$^{-/-}$). **E,** ELISA of IL-1β release by immortalized BMDM in iso- or hypo-tonic solution; n = 3 to 6 independent experiments. **F,** Relative macrophages (THP-1 or immortalized BMDM from C57BL/6, *Pycard*$^{-/-}$ or *Nlrp3*$^{-/-}$ mice) area after hypotonic stimulation at 0, 10 or 90 min, in the presence or absence of caspase-1 inhibitor Ac-YVAD-AOM (100 μM, 5 min before hypotonic solution). **G,** Western blot analysis of the cleavage of pro-caspase-1 to its active p10 subunit in HEK293 cells transfected with pro-caspase-1, ASC and NLRP3 full-length or NACHT-deleted NLRP3 (NLRP3-ΔNACHT) incubated for 1 h with hypotonic solution.

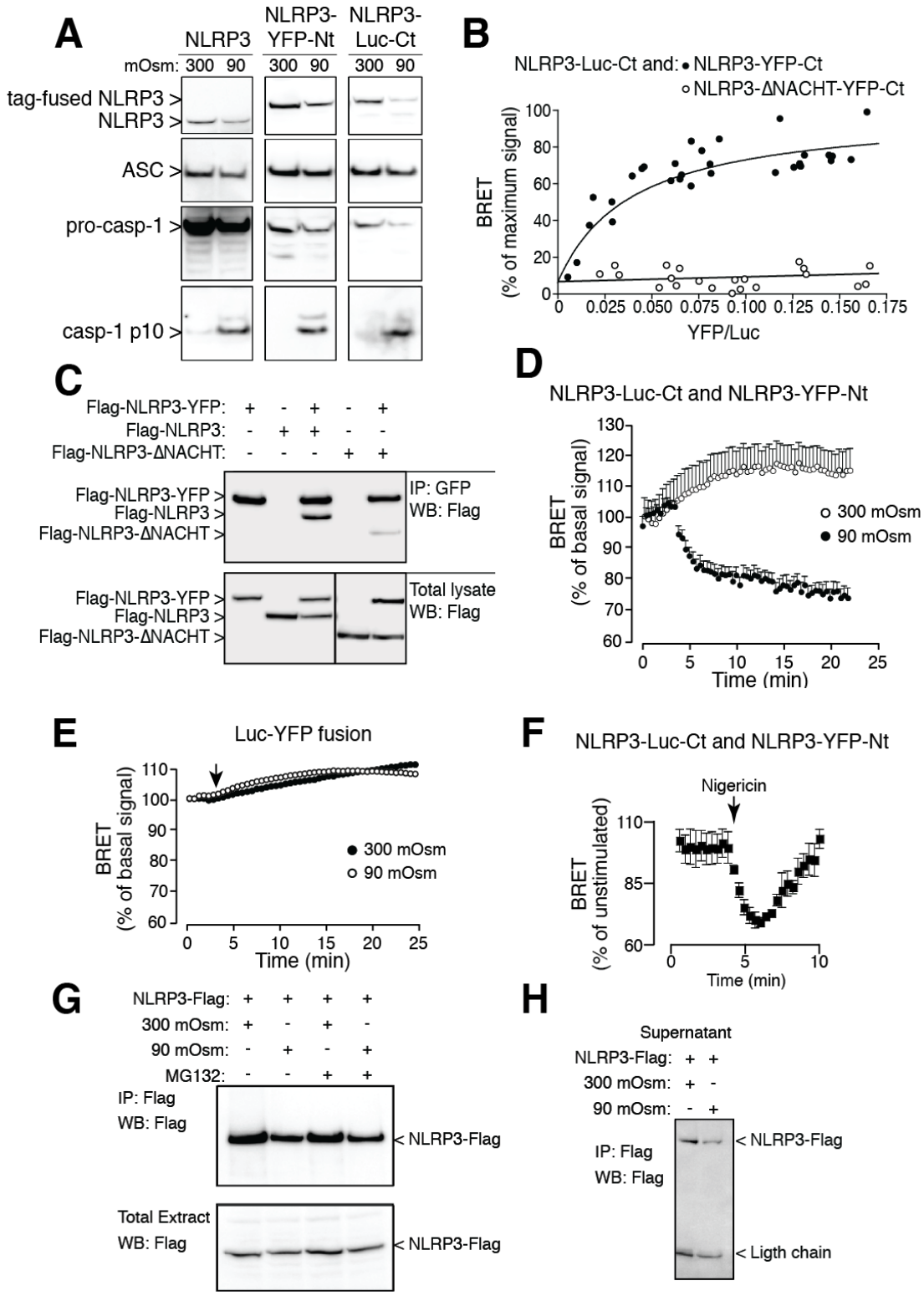

Figure S3. NLRP3 Conformational Changes in Response to Hypotonic Solutions
A, Western blot analysis of the cleavage of pro-caspase-1 to its active p10 subunit in HEK293 cells transfected with pro-caspase-1, ASC and the different BRET donor and acceptors of NLRP3, incubated for 1 h with hypotonic solution. **B**, BRET saturation curves for HEK293 cells transfected with a constant concentration of NLRP3-Luc-Ct

and increasing amounts of the BRET acceptor NLRP3-YFP-Ct (black circles) or NLRP3-ΔNACHT-YFP-Ct (open circles). **C**, Immunoprecipitation of full-length Flag-NLRP3-YFP when expressed alone or in combination with Flag-NLRP3 full-length or Flag-NLRP3-ΔNACHT. **D,** Kinetics of net BRET signal in HEK293 cells transfected with the BRET donor NLRP3-Luc-Ct and the acceptor NLRP3-YFP-Nt in response to iso- (open circles) or hypo- (black circles) tonic solution. **E,** Control kinetics of net BRET signal in HEK293 cells transfected with Luc-YFP fusion in response to iso- (closed circles) or hypo- (open circles) tonic solution. **F,** Kinetics of net BRET signal in HEK293 cells transfected with the BRET donor NLRP3-Luc-Ct and the acceptor NLRP3-YFP-Nt in response to nigericin (5 μM). **G,H,** Immunoprecipitation of NLRP3 before and after hypotonic stimulation with 90 mOsm solution in the presence or absence of proteasome inhibitor MG132 (10 min before and during stimulation, 50 μM). IP were carried out on solubilized cytoplasmic proteins (G) or on cell supernatants (H).

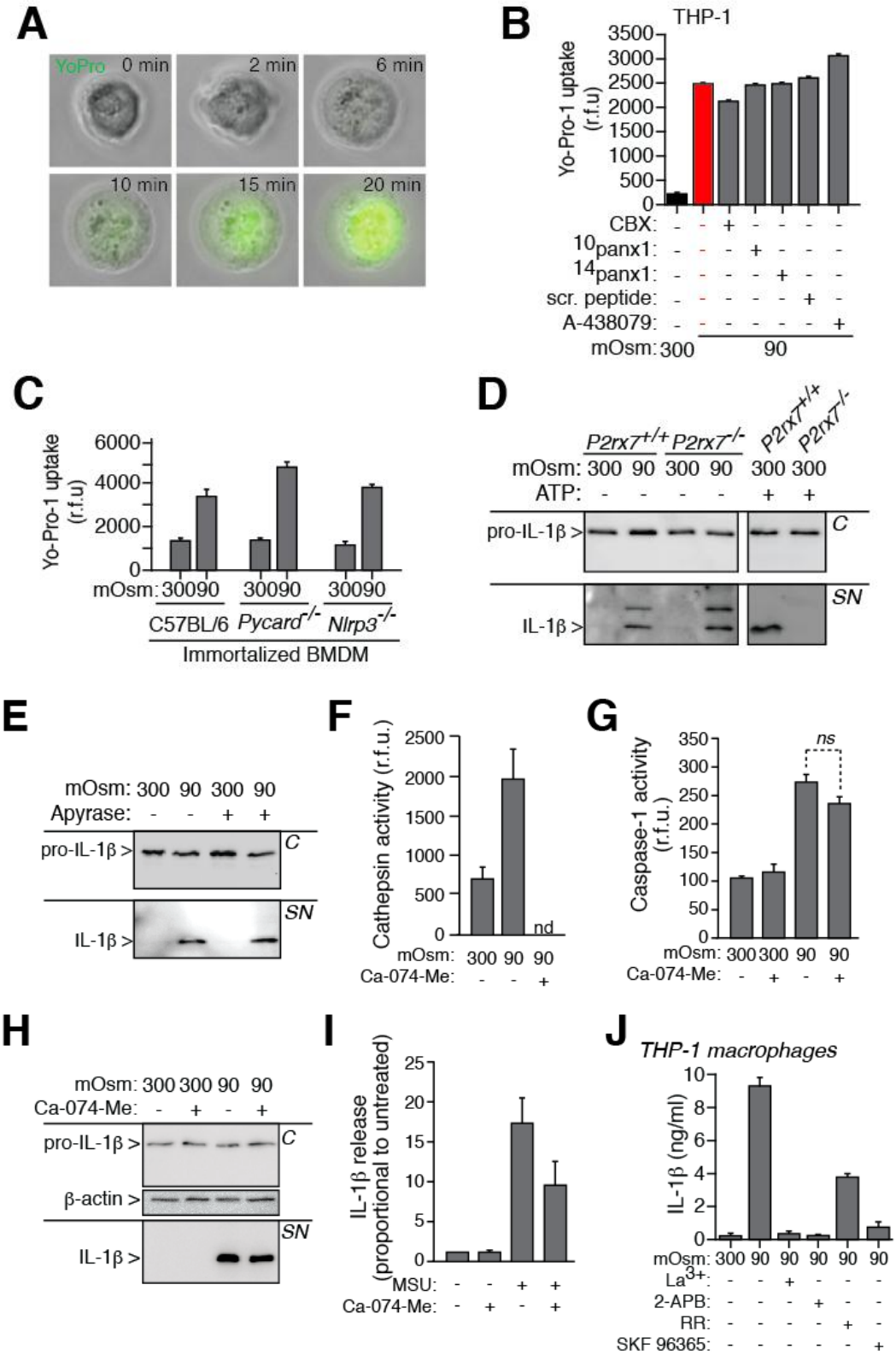
A
YoPro 0 min
2 min
6 min
10 min
15 min
20 min
B
THP-1
Yo-Pro-1 uptake (r.f.u)
3500
3000
2500
2000
1500
1000
500
0
CBX:
10panx1:
14panx1:
scr. peptide:
A-438079:
mOsm: 300 90
C
Yo-Pro-1 uptake (r.f.u)
6000
4000
2000
0
mOsm: 30090 30090 30090
C57BL/6 Pycard-/- Nlrp3-/-
Immortalized BMDM
D
P2rx7+/+ P2rx7-/- P2rx7+/+ P2rx7-/-
mOsm: 300 90 300 90 300 300
ATP:
pro-IL-1β >
C
IL-1β >
SN
E
mOsm: 300 90 300 90
Apyrase:
pro-IL-1β >
C
IL-1β >
SN
F
Cathepsin activity (r.f.u.)
2500
2000
1500
1000
500
0
nd
mOsm: 300 90 90
Ca-074-Me:
G
Caspase-1 activity (r.f.u.)
350
300
250
200
150
100
50
0
ns
mOsm: 300 300 90 90
Ca-074-Me:
H
mOsm: 300 300 90 90
Ca-074-Me:
pro-IL-1β >
C
β-actin >
IL-1β >
SN
I
IL-1β release (proportional to untreated)
25
20
15
10
5
0
MSU:
Ca-074-Me:
J
THP-1 macrophages
IL-1β (ng/ml)
10
8
6
4
2
0
mOsm: 300 90 90 90 90 90
La3+:
2-APB:
RR:
SKF 96365:

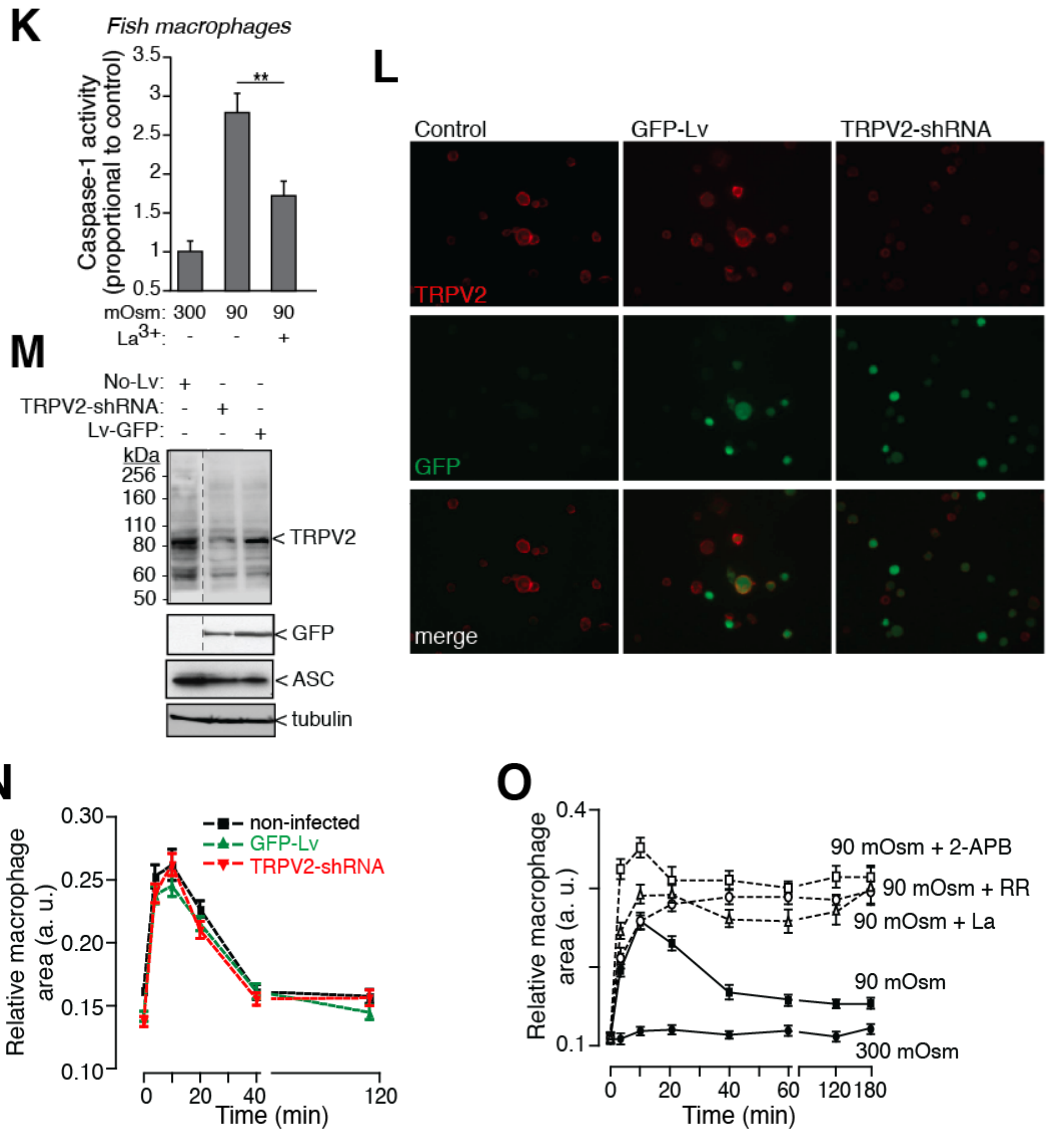

Figure S4. Hypotonic Stimulation of the NLRP3 Inflammasome Is Independent of P2X7 Receptor Activation but Dependent on TRP Channels

A, Kinetic of Yo-Pro-1 uptake in THP-1 cells during hypotonic solution stimulation. **B,C,** Yo-Pro-1 uptake in THP-1 cells (B) or from immortalized BMDM from C57BL/6, *Pycard*$^{-/-}$ or *Nlrp3*$^{-/-}$ mice (C) in response to 90 mOsm stimulation in the absence or presence of carbenoxolone (CBX, 100 μM), ^{10}panx1 mimetic peptide (1 mg/ml), ^{14}panx1 control peptide (1 mg/ml), scramble peptide (1 mg/ml) and P2X7 inhibitor (A-438079, 10 μM). **D,E,** Western blot of IL-1β release by mouse peritoneal macrophages from C57BL/6 (*P2rx7*$^{+/+}$) or *P2rx7*$^{-/-}$ mice primed with LPS (4h, 1 μg/ml) and incubated with hypotonic solution (40 min) or with ATP (3 mM, 30 min) (D) or by THP-1 treated as in A in the presence or absence of apyrase (5 units/ml, E); blots are representative of 2 to 3 independent experiments. **F,** Cathepsin B activity in the supernatants of THP-1 cells treated as in A using fluorogenic substrate (Z-RR-AMC). Incubation of these supernatants with the cathepsin B inhibitor Ca-074-Me (50 μM) completely blocked this activity; nd: not detectable; *n* = 3 independent experiments. **G,H,I,** Effect of cathepsin-B inhibitor (Ca-074-Me, 50 μM) on caspase-1 activation (G) or IL-1β release (H,I) by LPS-primed THP-1 in response to hypotonic stimulation (G,H) or MSU (I), *ns*: no significant p=0.0744 (*n* = 3

independent experiments). **J,** ELISA of released IL-1β by THP-1 cells primed with LPS (1 μg/ml, 4 h) and subsequently subjected to different extracellular osmolarities for 1h in the presence or absence of $LaCl_3$ (La^{3+}, 2 mM), 2-APB (100 μM), ruthenium red (RR, 100 μM) or SKF96365 (100 μM). **K,** Caspase-1 activity in fish macrophages induced by 1h of hypotonic solution in the presence or absence of $LaCl_3$ (La^{3+}, 2 mM); *n* = 6 to 9 independent experiments, **p = 0.0057. **L,** TRPV2 immunostaining in control THP-1, GFP-lentivirus infected cells (GFP-Lv) or in shTRPV2-lentivirus infected cells (TRPV2-shRNA). **M,** Immunoblot for TRPV2, GFP, ASC and tubulin in control THP-1, GFP-lentivirus infected cells (GFP-Lv) or in shTRPV2-lentivirus infected cells (TRPV2-shRNA). **N,O,** Relative THP-1 cell area in response to hypotonic solutions in control THP-1 (non-infected), GFP-Lv or in TRPV2-shRNA infected cells (N) or treated with different broad TRP inhibitors (O).

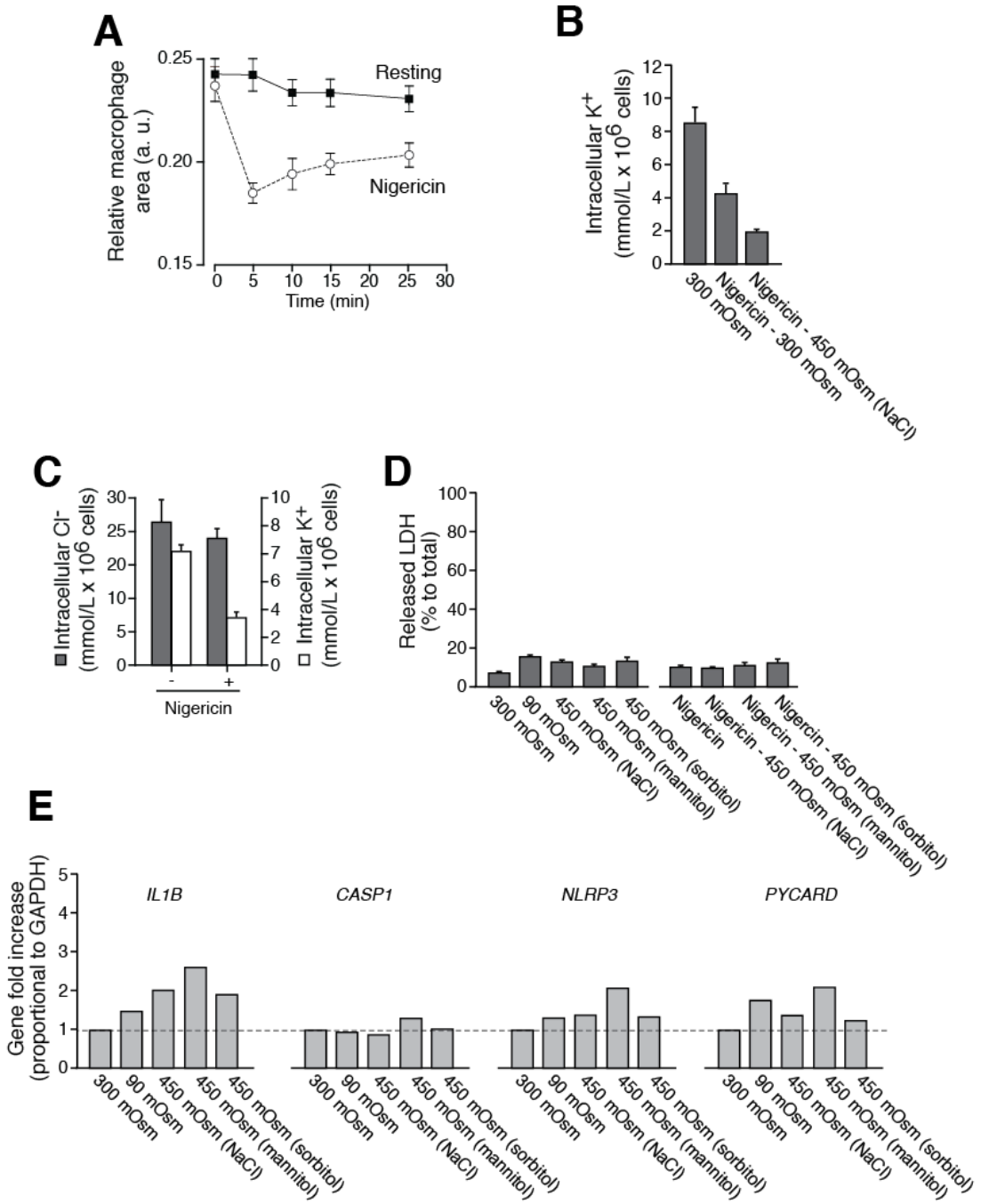

Figure S5. Nigericin Induces Cell Shrinking

A, Relative THP-1 cell area in response to 10 μM nigericin treatment for up to 25 min. **B,** Relative intracellular K^+ concentration of THP-1 treated as in A in iso- or hyper-tonic solution; *n* = 3 independent experiments. **C,** Relative intracellular K^+ and Cl^- concentrations of THP-1 treated with 20 μM nigericin for 30 min; *n* = 3 independent experiments. **D,** Percentage of released LDH in THP-1 cells treated with LPS (1 μg/ml for 4 h) and subjected to different osmolarities in the presence or absence of nigericin; *n* = 3 to 12 independent experiments. **E,** Relative *IL1B*, *NLRP3*, *PYCARD* or *CASP1* gene expression in THP-1 subjected to different extracellular osmolarities for 1 h after LPS priming.

Supplemental Experimental Procedures

Mouse Hippocampal and Human Macrophage Culture

Hippocampal cultures were prepared from 17,5 days embryonic mice (E17,5). At DIV3, media was supplemented by Cytosine β-D-arabinofuranoside hydrochloride 5mM (Sigma) for 12 hours. Neurons were studied between DIV12 and DIV14. Human peritoneal macrophages were obtained from laparoscopies where peritoneal lavage was performed before intervention for benign ovarian cyst removal and upon patient consent; macrophages were isolated by adherence to culture flask plastic and confirmed by flow cytometry using CD163 staining. Human peripheral blood monocytes (HPBM) were isolated from healthy donors following standard procedure using Limphoprep (Axis-Shield) and plastic adherence.

BRET Measurements

Transfected HEK293 cells were plated in poly-L-Lysine coated 96 well plate, after adhesion, cells were washed with PBS supplemented with 0.5 mM $MgCl_2$ and 1 mM $CaCl_2$ and readings were then immediately performed after addition of 5 µM coelenterazine-H substrate (Invitrogen) in iso- or hypo-tonic solution. Signals are detected with two filter settings (R-Luc filter, 485 ± 20 nm; and YFP filter, 530 ± 25 nm) at 37ºC using the Mithras LB940 plate reader (Berthold Biotechnologies). The BRET ratio was defined as the difference of the emission at 530 nm/485 nm of co-transfected R-Luc and YFP fusion proteins and the emission at 530 nm/485 nm of the R-Luc fusion protein alone. Results were expressed in milliBRET units (mBU). For saturation curves, a constant amount of R-Luc tagged proteins was transfected with

increasing quantity of YFP-tagged proteins. Amount of YFP- and R-Luc-tagged proteins was determined by reading on separate plates at 530 nm after cells excitation at 485 nm and reading at 485 nm in the presence of coelenterazine-H respectively. BRET signals were determined as described above. The BRET experiments have been performed using the ARPEGE Pharmacology Screening-Interactome platform facility at the Institute of Functional Genomics (Montpellier, France).

Supplemental Acknowledgments

Author contributions are as follows: V.C. contributed to the design, execution, analysis, and interpretation of the in vitro experiments in Figures 1B, 2C, 2D, 2G, 3A–3I, 4B, 4C, 4E, 4F, 5A, 5C, 5F, 5H–5K, 6C, 6F–6H, and 7H. A.B.-M. and C.M.M. performed and analyzed the in vivo models in Figures 1C–1F and 7A–7D. A.B.-M., G.L.-C., and A.I.G. performed and analyzed the experiments in Figures 1A, 2A, 2B, 2F, 4A, 4D, 4G, 5B, 5D, 5E, 5G, 6A, 6B, 6D, 6E, and 7E–7G. D.A. and V.M. designed, performed, and analyzed the fish experiments in Figure 2E. M.T.M., A.S.H., E.B., and D.R. designed, performed, analyzed, and interpreted the kainic acid model in Figure 7I. J. P.P. conceived, designed, and supervised this study, analyzed and interpreted results, and wrote the final manuscript with V.C. and with contributions from the other authors.